National Radio Astronomy Observatory
Socorro, New Mexico
Very Large Array Program

VLA Test Memo No. 158

Spectral Dynamic Range at the VLA: The 3 MHz Ripple

C.L. Carilli
October, 1991

I. Introduction

Bandpass calibration at the VLA normally involves scans on a bright continuum point source, from which the spectral channel dependence of the complex gains of each antenna are determined (Rots 1988, van Gorkom and Ekers 1985, Clark and van Gorkom 1981). These antenna based spectral response functions, or 'bandpasses', are then used to correct the target source spectrum for gain variations across the spectral band. Since target source and calibration source scans are not simultaneous, any temporal variation in these bandpasses will lead to residual errors in the corrected target source spectrum. In particular, such bandpass gain errors lead to residual errors in the spectrum of any continuum source in the target field.

At the VLA, the dominant residual error after bandpass calibration is a sinusoidal ripple with a period of about 3 MHz. For observations made with bandwidths of 3 MHz or larger, this ripple typically limits spectral dynamic range to a few hundred. We define spectral dynamic range as:

Spectral Dynamic Range = (Continuum Flux Density)/(peak-to-peak of Residual Ripple in Source Spectrum).

The current best guess is that the 3 MHz ripple in the antenna based bandpasses is due to a standing wave in the waveguide system between the B rack modem and the coupler into the main waveguide (Clark, Bagri, Palmer, van Gorkom, *priv. comm.*). This guess is based on the fact that the waveguide pathlength between these 2 devices is roughly consistent with the observed period of the standing wave. Of course, it is not the standing wave in the spectral response function that is the problem, but the variation of this wave with time that leads to residual gain errors after bandpass calibration.

It is the purpose of this memo to both quantify and monitor bandpass problems due to this ripple, and to delineate an interim solution to the problem. We say interim since the problem will disappear when the VLA IF system is upgraded to include samplers at each

antenna and/or an optical fiber IF transmission system. A list of the important conclusions from these tests, and a proposal list for future testing, is given in section V.

II. Test Observations

An observing log for the test observations is given in table 1. Each observing run entailed a series of 10 to 15 minute scans on 3C 286 (1331+305), spaced over a period of 2 to 3 hours. All observations were made using correlator mode 1A, bandwidth code 3, and on-line hanning smoothing. The resulting spectra had 63 spectral channels, with a channel width of 97.7 kHz, and a total spectral range of 6.25 MHz. The observing frequency for each run was 1406 MHz. The flux of 3C 286 at this frequency is 14.9 Jy.

The data were amplitude and phase self-calibrated in AIPS. Then antenna based bandpass solutions were determined for each scan on 3C 286 using BPASS. The antenna based bandpass solutions were examined for each scan using the program POSSM. Also, in order to investigate the change in these bandpass solutions as a function of time, a special AIPS program, POSSD, was written. POSSD takes the antenna based bandpass solutions for a specified antenna, and for two specified time ranges, and determines the temporal variation of the bandpass between these two times by dividing the amplitude solutions from the first time range, by those from the second, and by subtracting the first set of phase solutions from the second. Hence POSSD determines the fractional change in the gain of a given channel between 2 specified time ranges for a given antenna.

We hereafter define the 'amplitude variance' for a given antenna as: *amplitude variance = the maximum fractional change of the channel dependent gains for a given antenna's bandpass between two specified scans.* This is determined from the peak-to-peak amplitude on plots produced by POSSD. The POSSD routine allows for an easy study of the variation of the shape of the bandpass for each antenna as a function of time.

We note that throughout this memo there are shown 3 types of plots which look similar, but aren't. First, there are source spectra, produced from vector averaging of the visibility data after bandpass calibration. Second, there are antenna based bandpass solutions for given scans. And third, there are bandpass variance plots, which show the fractional change of the antenna based bandpass response function between two scans, as described above. The text and the figure captions state clearly which type of plot is displayed.

III. Results

A. The Problem

We start with an example of a particularly bad spectrum of a bright continuum source resulting from standard VLA bandpass calibration, as shown in figure 1. This spectrum was

made from data taken during the A/B array observations. It was produced by applying the averaged antenna based bandpass solutions (averaged over all the scans on 3C 286, covering a total span in time of 150 minutes), to the data from one 10 minute scan on 3C 286. The spectrum was produced using vector averaging of the visibilities. Notice the clear sinusoidal ripple with a period of 3.2 MHz. The peak-to-peak amplitude variation is 0.12 Jy, implying a spectral dynamic range of 125 for this spectrum.

B. Which Antennas Are Bad?

For illustration, figure 2 shows bandpass variance plots for 3 antennas from the A array observing run, determined from 2 scans on 3C 286 separated by 30 minutes. For antenna 24 (figure 2A) we find very little variation in the shape of the bandpass over time. The amplitude variance is less than 0.4%. For antenna 7 (figure 2B) we find a moderate temporal variation in the antenna bandpass, with an amplitude variance of about 0.6%. For antenna 12 (figure 2C) we find a large change in the bandpass between scans, with an amplitude variance of 3.0%.

Such bandpass variance plots were analyzed for each antenna for each observing run. In table 2 we summarize the results. Column 1 lists the antenna number. Column 2 lists the results from the D array experiment for the amplitude variance of each antenna. The variance 'quality' codes are as follows: G means good, or an amplitude variance of less than 0.4%. M means moderate, or an amplitude variance between 0.4 and 0.8%. B means bad, or an amplitude variance in excess of 0.8%. Column 3 lists the antenna station for the D array observations. Columns 4 and 5 give the same data for the A array experiment, columns 6 and 7 give the same data for the A/B array experiment. In each case the variances were calculated from two scans on 3C 286 separated by 30 minutes. For the bad antennas, the value of the amplitude variance is listed in parentheses.

The quality of the variance in phase is not listed. We find that antennas which show large amplitude variances also show large phase variances (peak-to-peak phase variances $>>$ 0.4^o), while good antennas are usually good in both amplitude and phase (peak-to-peak phase variances $< 0.4^o$).

The majority of the antennas fall into the G or M category, implying variances less than 0.8%. More importantly, inspection of the variance plots for the bad antennas shows that, when an antenna is bad, it is typically very bad, with a peak-to-peak amplitude variance in excess of 1%.

C. Is the Problem Antenna Based or Station Based?

The data in table 2 can be used to address the question of whether the problem is antenna dependent, or station dependent. This question arises because the internal waveguide

reflections thought to be causing the standing waves could be occurring primarily at the modem, which is in the vertex room of the antenna, or at the coupler to the main waveguide, which is in the man-hole at each station.

The fact that antenna 12 was moved twice, and yet remained bad, is very clear evidence that the problem can be antenna based. However, there are also examples of antennas which went from good to bad (antenna 17) or bad to good (antenna 2) after being moved. This suggests that the problem can also be station dependent. Further monitoring is required to verify whether stations as well as antennas can be bad.

D. What is the Timescale for Bandpass Variations?

In figure 3 is plotted the gain of selected channels as a function of time for data taken during the A/B array experiment. Data is plotted for a good antenna (antenna 14, lower plot) and a bad antenna (antenna 12, upper plot). The zero point in time corresponds to the middle of the first scan, or LST = 15:05. The upper set of points in each plot shows the gain of channel 16, while the lower set of points shows the gain of channel 32 for each antenna.

For the good antenna, the gain variation is zero to within the noise. For the bad antenna, the gain variation for a given channel over the full time range is large. However, it is clearly *a smooth function of time.* We should point out that the antennas were moved off-source by over 30° between scans for the final 4 scans, with no noticeable change in the smoothness of the temporal gain variation.

E. What Causes a Large Bandpass Variance?

Figures 4A and 4B show the bandpass variances for a bad antenna (antenna 12) and a good antenna (antenna 14) between two scans separated by 136 minutes, for data taken from the A/B array observing run. The bad antenna shows an amplitude variance between these two scans of 15%. The good antenna shows an amplitude variance less than 0.4%.

In figures 5A and 5B is shown the bandpass solutions for antenna 12 for the two individual scans from which the variance plot of figure 4A was determined. Figures 5C and 5D show the corresponding data for antenna 14. The peak-to-peak change in amplitude across the band for antenna 14 is 6% in both scans, while that for antenna 12 is 15% in both scans. We see that, while the amplitude variance between these two scans was a factor of 40 larger for antenna 12 than for antenna 14, the magnitude of the peak-to-peak variation of the gain across the band differs by only a factor of 3 between the good and bad antennas.

So what causes the large variance for antenna 12? Notice that the position of the 'standing wave' in the bandpass for this antenna (see figures 5 A and B) shifts in phase by about 10 channels between these two scans. The large variance in the bandpass of antenna 12 (see figure 4 A) between these two scans is therefor due to a *shift in phase of the standing*

wave in the antenna based spectral response function over time.

This point is illustrated in figure 6. We follow the phase of the standing wave in antenna 12 as a function of time by plotting the channel of the peak of the bandpass versus time for data taken from the A/B array observations. Two data sets are plotted, corresponding to the 2 peaks observed in the bandpass (see figure 5 A). The variation in phase of the standing wave appears to be smooth with time, with a slope of about 3.8 channels per hour, or 375 kHz per hour. The slope is the same for both peaks. During these observations the peak-to-peak amplitude of the standing wave response function, the period of the standing wave, and the shape of the standing wave, remained constant over time (see figure 7). Note that the gain variations plotted in figure 3 are a direct result of this shifting in phase with time of the standing wave in the spectral response function of antenna 12.

IV. Some Interim Solutions

The first encouraging result is that the bandpass standing wave variance problem is usually severe in only a few antennas in a given observation. The most obvious thing to do then, is to flag the bad antennas. The effect of flagging the bad antennas is shown in figure 8. This is the same spectrum as figure 1, produced in the same way, but now the three bad antennas from table 2 (column 6) have been flagged. The peak-to-peak variation in amplitude across the band is lower by a factor of 6 than that of figure 1, implying a spectral dynamic range of 750.

The second encouraging result is that the gain variation for a given channel seems to be smooth with time, even in the worst antennas. This suggests that even bad antennas may be salvageable through interpolation of antenna based bandpass solutions between calibrator scans. For a linear interpolation of the bandpass between calibrator scans to work, the required minimum time between calibrator scans is governed by the timescale on which the changes in gain remain roughly linear. From figure 3, it appears that departures from linearity occur on timescales larger than about 30 minutes. Hence, calibrating every 30 minutes or less should allow for reasonable bandpass interpolation.

We demonstrate this solution in figure 9. This is the same spectrum as figure 1, but now the bandpass has been determined by interpolating between the solutions from the scan directly before and the scan directly after the 'target source' scan. The time separating bandpass solutions is then 20 minutes. The spectral dynamic range for this spectrum is 500/1, or an improvement by a factor of 4 from figure 1, even with the bad antennas included.[1]

---

[1] Note that the required time spent on each bandpass calibration scan is set only by the amount of time on the target source between calibration scans, and not by the total observing time on target source. A reasonable rule of thumb to insure that the signal to noise on the target source is not dominated by bandpass calibration is: $t_c = 9 \times (S_t/S_c)^2 \times t_t$, where $t_c =$

The 'final solution' is shown in figure 10. This spectrum combines the flagging procedure of figure 8 with the bandpass interpolation procedure of figure 9. There is the suggestion of a ripple at a level of 0.01 Jy peak-to-peak, but this is only two times larger than the expected thermal noise. The implied spectral dynamic range is $\geq$ 1500/1. Overall, we have gained by a factor of at least 12 in spectral dynamic range from the most naive solution of figure 1.

Figure 11 summarizes the four stages of improvement. Part A is the original spectrum (figure 1). Part B is the spectrum after flagging bad antennas (figure 7). Part C is the spectrum after interpolation of the bandpass between the nearest scans, without flagging bad antennas (figure 8), and part D is the final spectrum, including flagging and bandpass interpolation (figure 9).

V. Summary and Future Tests

The main points of this memo are:

1) The dominant limitation to high spectral dynamic range with the VLA for observations with total bandwidths $\geq$ 3 MHz, appears to be a sinusoidal ripple in the antenna based bandpass spectral response functions. The period of the ripple is about 3.2 MHz, which is consistent with it being a standing wave in the waveguide between the B rack modem in the vertex room and the coupler into the main waveguide.

2) The problem can be antenna dependent for certain, but may also be station dependent.

3) For a given observation, antennas fall into 2 categories: either the amplitude variance between scans separated by 30 minutes in time is small (amplitude variance $\leq$ 0.6%), or large (amplitude variance $\geq$ 1%). The vast majority of the antennas fall into the first category.

4) The gain variation of a given channel for a 'bad' antenna is smooth with time, with the time constant for significant variations being about 30 minutes.

5) This temporal gain variation for a give channel in a 'bad' antenna is not due to a change in the amplitude, the period, or the shape, of the standing wave, but arises from a roughly linear change in phase of the standing wave with time. The slope in time for the shifting phase for the bandpass of antenna 12 for the A/B array observations was 375 kHz per hour.

6) Points 3 and 4 suggest that through flagging of bad antennas, and by interpolating the bandpass over timescales shorter than about 30 minutes, one can increase the spectral dynamic range of the final spectrum. Our tests show that at an order of magnitude im-

---

calibration source scan time, t_t = target source scan time, S_t = target source continuum flux density (or peak surface brightness), S_c = calibration source continuum flux density. The factor of 9 implies that the signal to noise on calibrator is a factor of 3 higher than that on source, per scan. This equation holds for $S_t << S_c$. For the case of $S_t \approx S_c$, then equal time is needed on bandpass calibrator and on target source to maximize signal to noise.

provement can be made using these techniques. Note that this requires proper set-up of the observe file, with frequent scans on calibrator. Spectral dynamic ranges in excess of 1000/1 are obtainable with these techniques.

There are a number of tests which could be performed to better understand, and perhaps correct, this problem.

1) We should look at the hardware of a bad antenna and station. Perhaps there are some obvious defects in either the coupler or the modem which could be fixed?

2) We should continue to monitor the quality of the antennas through the next two array changes (C and D). This should provide clues into the station dependence of the standing wave problem.

3) We should look at the elevation and temperature dependence of the problem.

We conclude with a few remarks. The first is that the problem is fairly fickle, in that sometimes the array works very well, and sometimes not. Test 3 may shed light as to why this is, and procedure 6 should allow for fairly high spectral dynamic range observations to be made in even the worst conditions. The second is that a real time bandpass calibration routine, as outlined by Thompson (1978), might alleviate this residual standing wave problem. The third is that post-processing continuum subtraction routines such as UVLIN (Cornwell, Uson, and Haddad 1991), which remove linear baselines fit to the spectrum of each visibility, will have no impact on the sinusoidal effects described herein. And last, in theory the 3 MHz standing wave should be observing band independent, since it's an IF problem. Tests should be done to verify this.

Appendix: Auto-Normalization

The VLA provides the option of 'auto-normalization', or normalizing the observed cross correlated spectra in real time by using the autocorrelation spectrum from each antenna (Clark and van Gorkom 1981). In theory, such a process should remove temporal variations in antenna based gains. In practice, a number of problems arise using this process (Rots 1988).

First, no correction is made to the channel dependent phases. Hence, bandpass phase calibration needs to be done in the usual way, as described in section I.

Second, for observations with 'strong' line signal in the single dish spectrum (either in absorption or emission), the single dish bandpass will be corrupted. In this case, 'strong' is measured relative to the system temperature. As a rough rule of thumb, the single dish line signal limit is:

$$G \times S_{SD} < T_{sys}/SDNR,$$

where G is the antenna gain (K/Jy), S_{SD} is the single dish line flux (Jy), T_{sys} is the system

temperature (K), and $SDNR$ is the required spectral dynamic range. For instance, for the VLA in L band, $G \sim 0.1$ K/Jy and $T_{sys} \sim 50$K. Hence, a single dish line signal of 100 mJy is large enough to limit spectral dynamic to 5000/1 when employing auto-normalization.

And third, there is the problem of interference. Phase incoherence of terrestrial interference signals provides an interferometer with 'natural' interference rejection. However, when using auto-normalization, the response of a single dish to interference is put back into the data. This can lead to obvious problems when working outside the protected bands.

We have performed tests to see whether auto-normalization allows for higher spectral dynamic range with the VLA. Observations where made in B array, and the observing and analysis procedure outlined in section II was applied to the auto-normalized spectra. As a comparison, observations without auto-normalization were made during the same observing run. We note that about 1/3 of the data with auto-normalization applied had to be flagged due to interference. The results are shown in figures A1 and A2. Figure A1 shows bandpass variance plots for antennas 12 and 3. Parts A and B are variances with auto-normalization applied, while parts C and D are variances without auto-normalization. The time between scans for the variance calculations was 30 minutes. Notice the pronounced 'ripple' in the bandpass variance of antenna 12 without auto-normalization (A1, part C). This amplitude ripple is completely removed when applying auto-normalization (A1, part A). The phase ripple remains unchanged with or without auto-normalization, as expected. For antenna 3, the auto-normalized bandpass variance (A1, part B) shows a slope in variance of about 1% across the band, while the variance without auto-normalization (A1, part D) is flat to within the noise (note that antenna 3 was the phase reference antenna).

Figure A2 shows spectra of 3C 286 made employing the techniques outlined in section IV, for data obtained with and without auto-normalization. The expected 'noise' in these spectra is 5 mJy/beam, hence the theoretical maximum SDNR is 3500/1. For the data without auto-normalization (A2, part A), we find a residual slope across the band of amplitude $\sim$ 15 mJy, implying a spectral dynamic range of $\sim$ 1000/1. For data with auto-normalization, we see a slight upturn in the bandpass toward higher channels, with amplitude $\sim$ 10 mJy, implying a SDNR $\sim$ 1500/1.

We conclude that auto-normalization can remove the time variable 3 MHz ripple in amplitude for the channel dependent gains for a given antenna, but that it may introduce other effects in the bandpass variance which are not understood, and need to be investigated (see figure A1). The resulting spectrum with auto-normalization has slightly higher spectral dynamic range than the spectrum without auto-normalization, but only by-about 50%. Given that relatively high SDNR can usually be obtained without auto-normalization through the techniques described in section IV, and that phase corrections require the usual procedure of bandpass calibration using a strong calibrator anyway, and especially that the potential for data loss due to interference is dramatically worse when auto-normalization is employed, we

would recommend not using the auto-normalization option for the vast majority of experiments.

References

Clark, B.G. and van Gorkom, J.H. 1981, VLA Test Memorandum No. 131.

Cornwell, T.J., Uson, J.M., and Haddad, N. 1991, *A. and A.*, in press.

Rots, Arnold 1988, *A Short Guide for VLA Spectral Line Observers.*

Thompson, A.R. 1978, VLA Electronics Memorandum No. 172.

van Gorkom, J.H. and Ekers, R.D. 1985, *Synthesis Imaging*, eds. Perley, R., Schwab, F., and Bridle, A., NRAO, Greenbank, WV, p. 177.

Table 1: Log of Test Observations

Array	Date	Start Time (LST)	Stop Time (LST)
D	4/28/91	14:30	16:00
A	9/2/91	11:00	13:00
A/B	9/24/91	12:00	15:00
B[a]	11/1/91	10:30	13:30

[a] Tests of on-line auto-normalization were made during the B array observations (see appendix).

Table 2: Variance Codes From Test Observations

Antenna	D array Variance	Station	A array Variance	Station	A/B Array Variance	Station
1	G	W5	G	W32	G	W32
2	B (1.0%)	N6	G	N56	G	N56
3	M	W2	M	W40	G	W4
4	G	E2	M	E32	G	E32
5	G	E6	G	E56	G	E28
6	G	N5	G	N48	G	N48
7	G	E9	M	E72	G	E72
8	M	N7	G	N64	–	–
9	G	W8	G	W8	–	–
10	G	W1	G	W24	G	W24
11	G	W3	M	W48	M	W12
12	B (1.2%)	W9	B (3.0%)	W72	B (3.0%)	W36
13	–	–	G	N24	M	N24
14	G	E5	M	E48	G	E20
15	G	N9	G	N72	G	N72
16	G	E1	G	E24	G	E24
17	G	N4	B (2.0%)	N40	B (2.0%)	N40
18	G	E4	G	E40	G	E12
19	M	W4	G	W56	M	W20
20	M	W7	B (2.0%)	W64	B (1.0%)	W28
22	–	–	M	E64	–	–
23	G	E8	G	E8	G	E8
24	G	E3	G	E16	G	E16
25	–	–	G	N16	G	N16
26	M	N2	M	N32	G	N32
27	M	N3	–	–	–	–
28	G	W6	M	W16	G	W16

Figure 1: The radio continuum spectrum of 3C286 at 1406 MHz. This spectrum was produced from the A/B observations, using vector averaging of all the visibilities, and using an average bandpass determined from all the data. The channel width is 97.7 kHz.

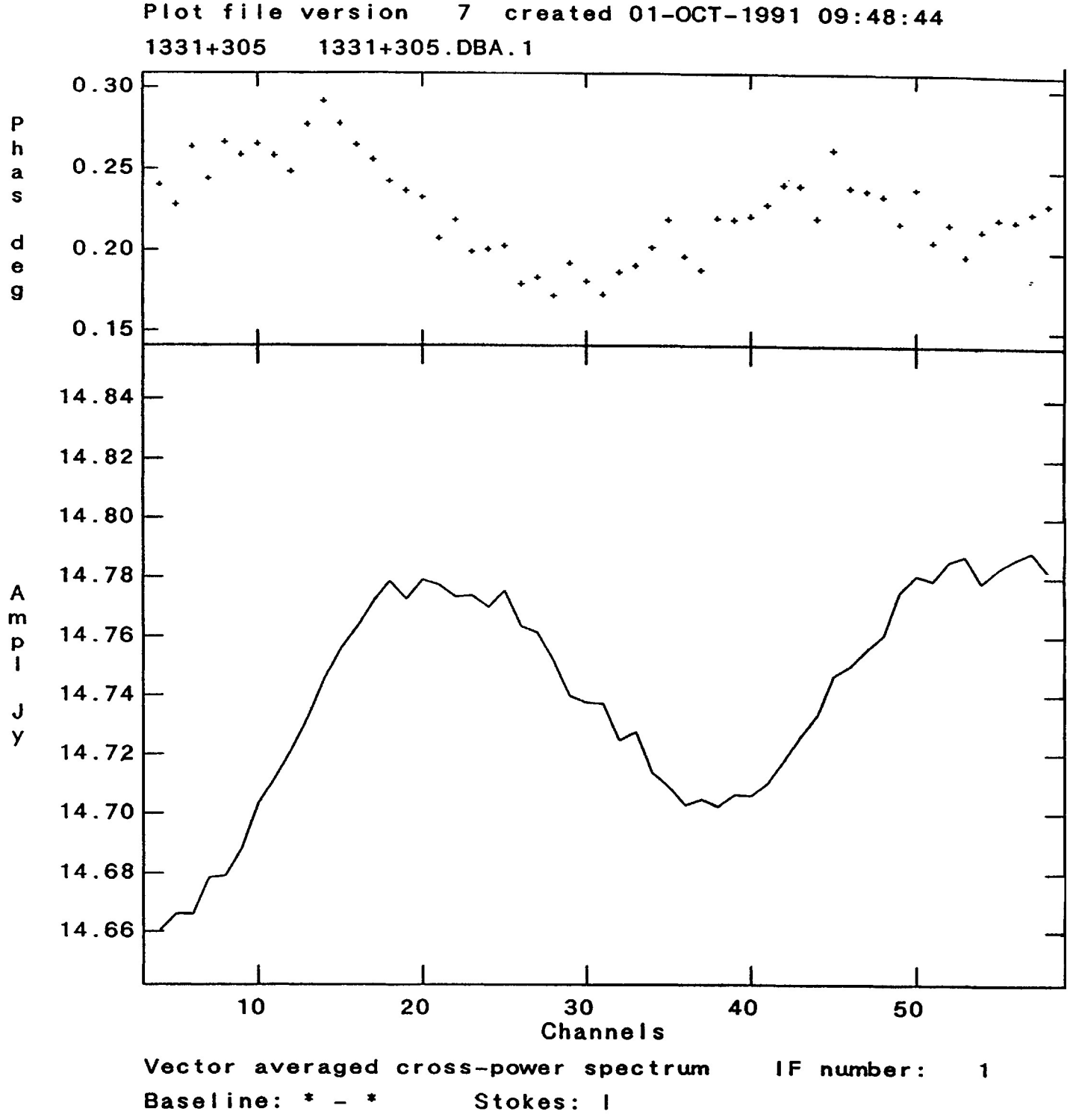

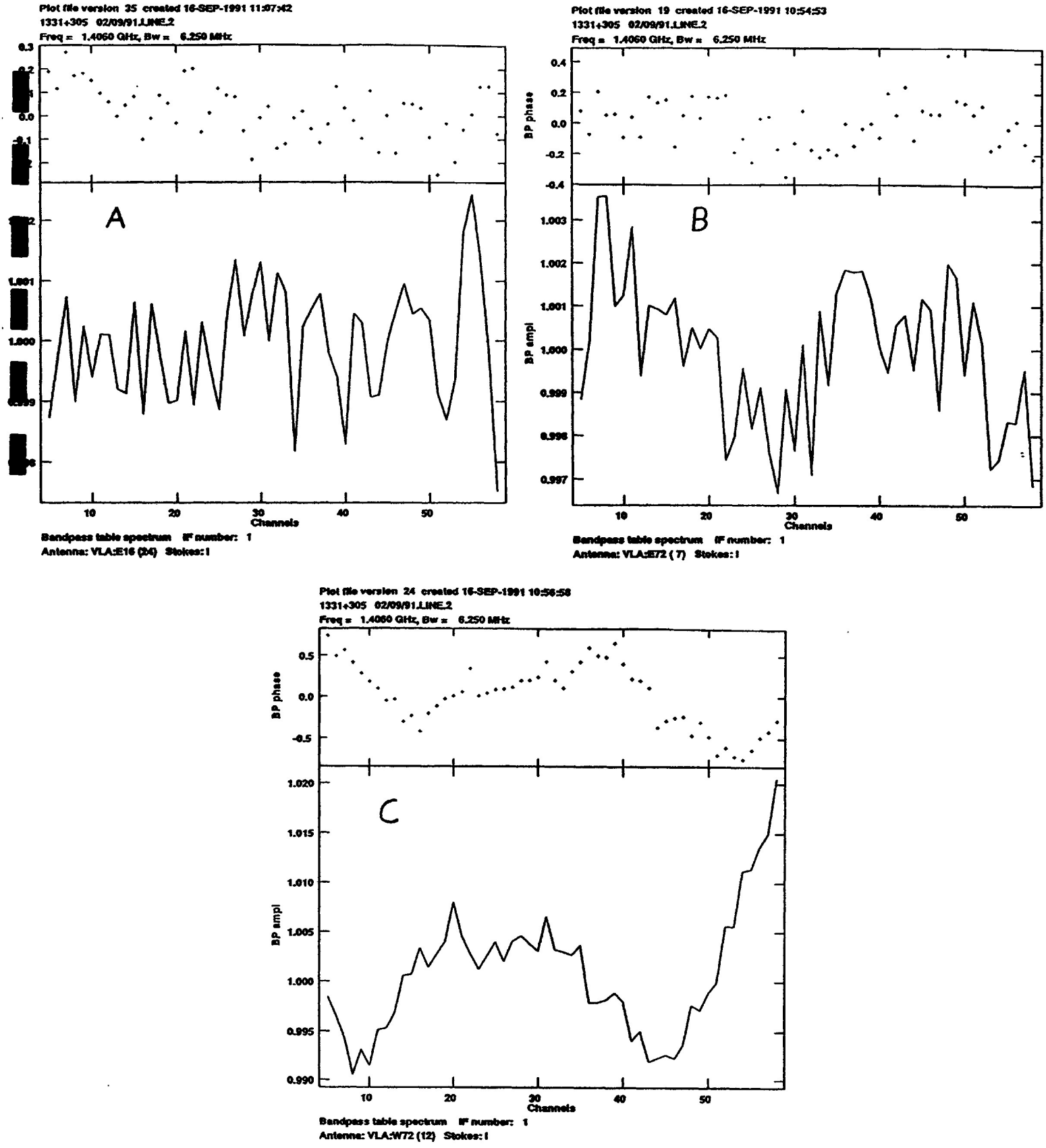

Figure 2: Examples of 'bandpass variance' plots produced by the POSSD program from the A array observations, as described in section II of the text. These variances were taken between 2 scans separated by 40 minutes. Figure A is for antenna 24 (a Good antenna). Figure B is for antenna 7 (a Moderate antenna). Figure C is for antenna 12 (a Bad antenna). Note the scale change between various plots.

Figure 3: The temporal behavoir of the gain in selected channels as a function of time. The channel gain plotted is the amplitude of the antenna based, channel dependent, gain solutions determined by BPASS. Each point is the solution from an individual 10 minute scan, taken from a series of scans on 3C 286 during the A/B array observations. Channels 16 and 32 are plotted for antennas 12 and 14.

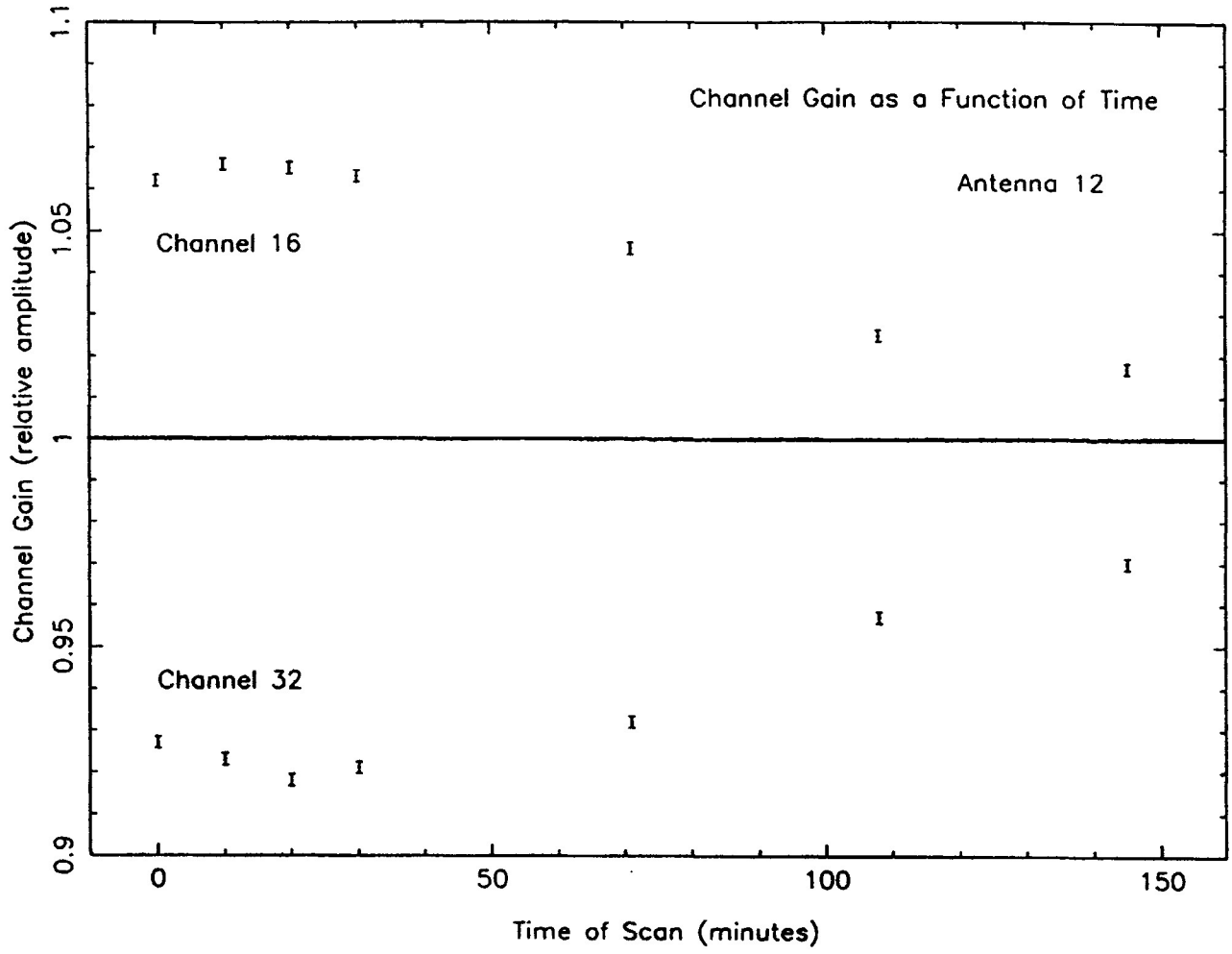
Channel Gain as a Function of Time
Antenna 12
Channel 16
Channel 32
Channel Gain (relative amplitude)
Time of Scan (minutes)
1.1
1.05
1
0.95
0.9
0
50
100
150

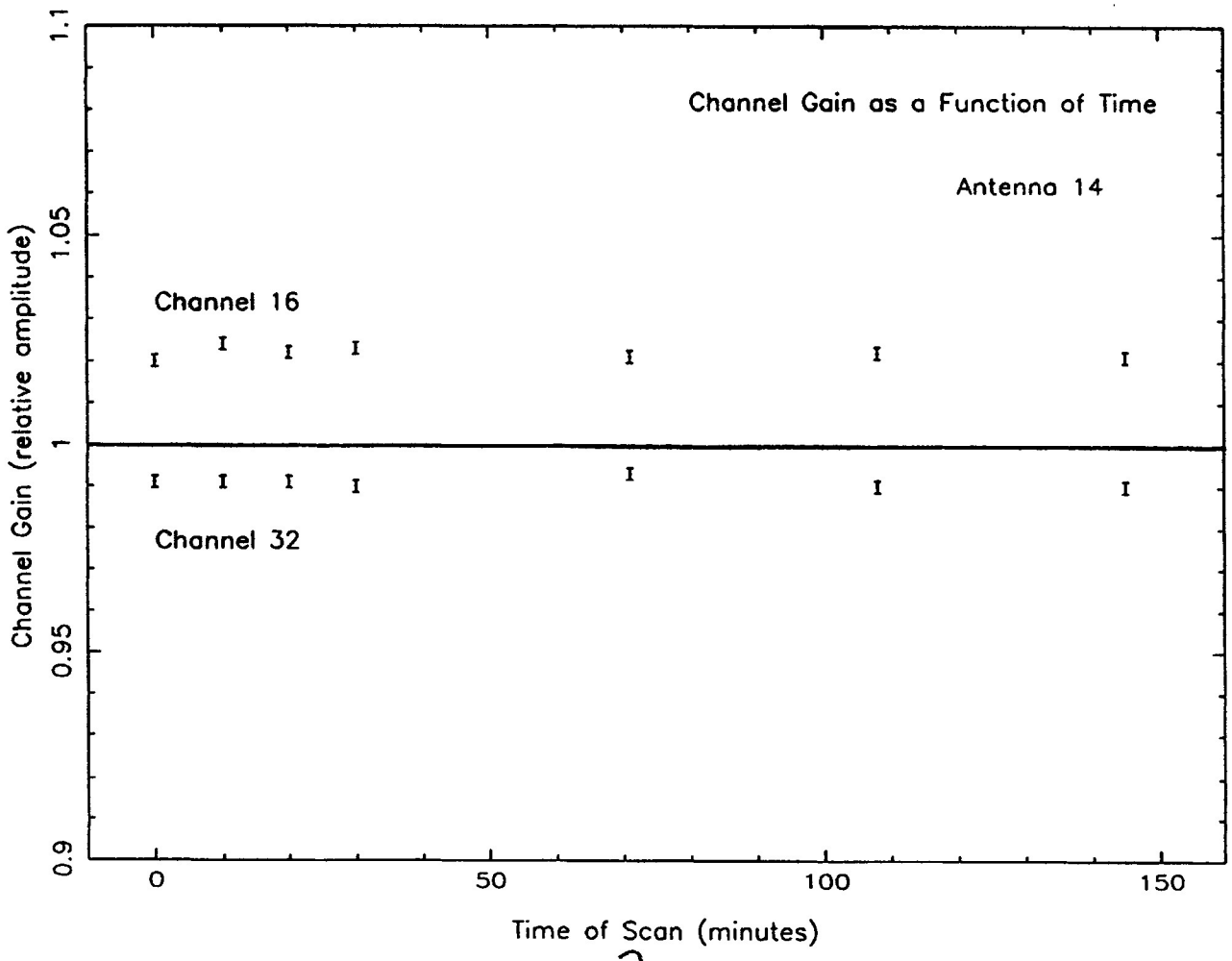
Channel Gain as a Function of Time
Antenna 14
Channel 16
Channel 32
Channel Gain (relative amplitude)
Time of Scan (minutes)
1.1
1.05
1
0.95
0.9
0
50
100
150

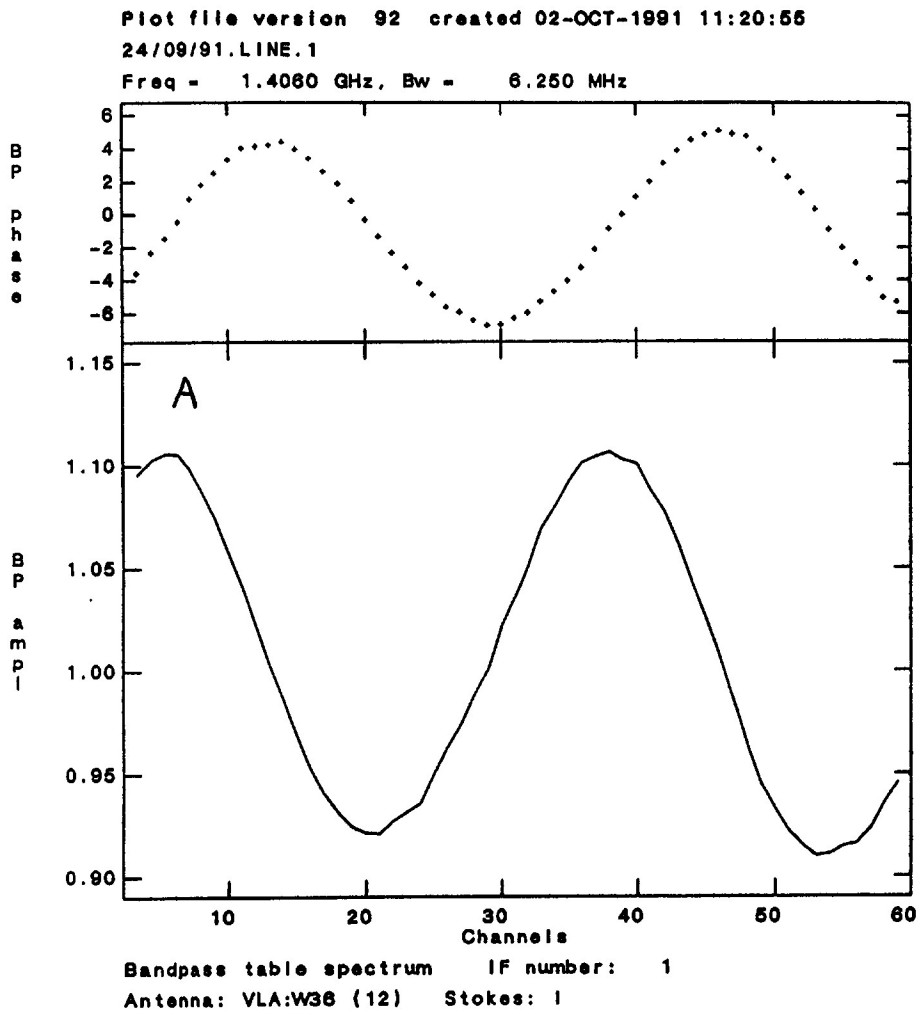

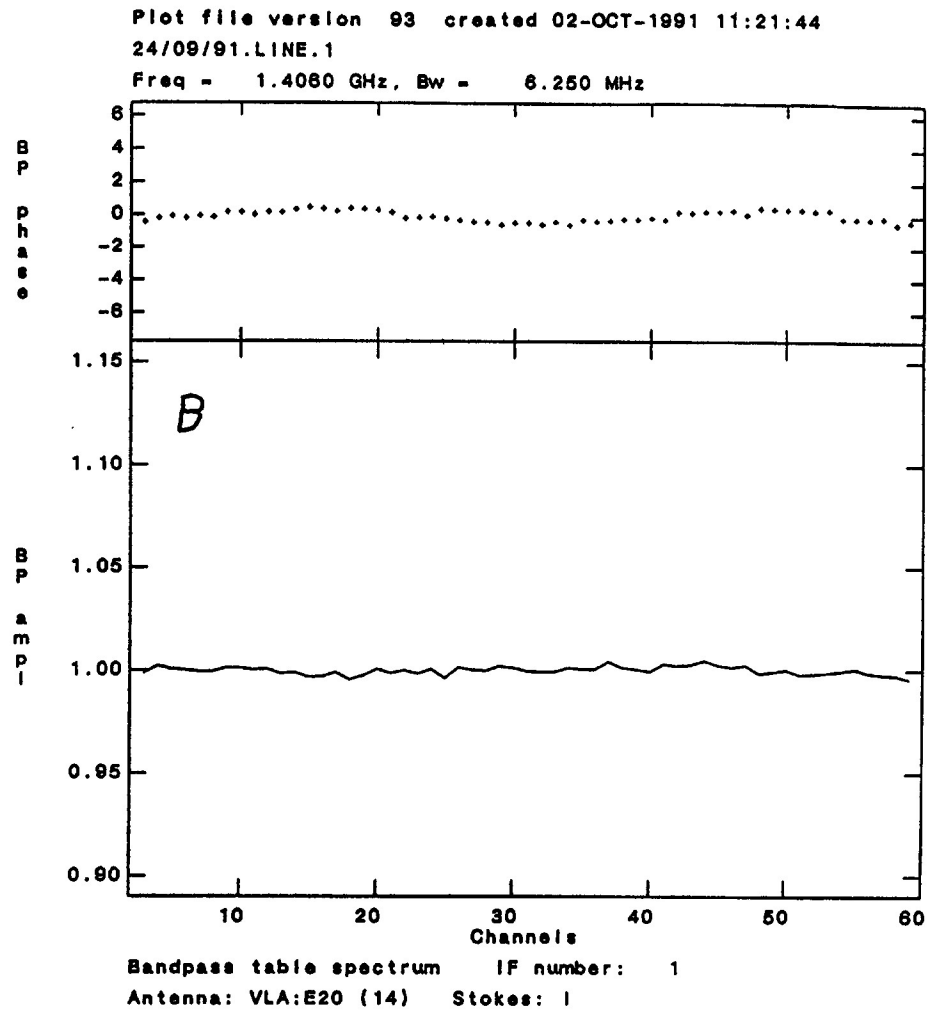

Figure 4: A. The bandpass variance for antenna 12 between 2 scans separated by 136 minutes in time, from data taken during the A/B array observations. B. Same as A but for antenna 14.

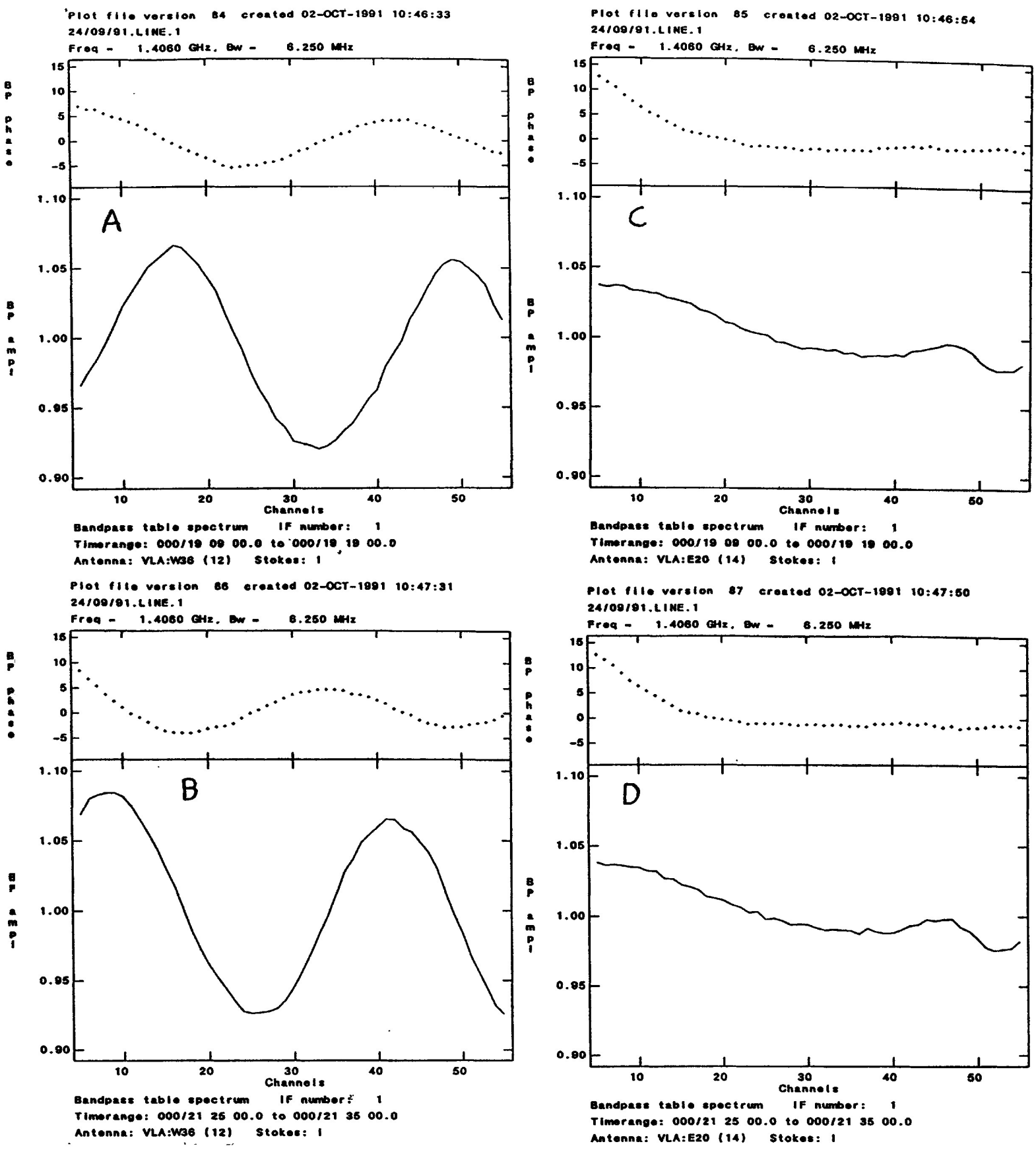

Figure 5: The bandpass solutions for the two scans used to determine the variances in figure 4. Figure A shows the bandpass solution for antenna 12 for the first scan. Figure B shows the bandpass solution for antenna 12 for a scan 136 minutes later. Figure C shows the bandpass solution for antenna 14 for the first scan. Figure D shows the bandpass solution for antenna 14 for a scan 136 minutes later. Notice the shift in phase of the standing wave in the bandpass of antenna 12 between scans. It is this phase shift which gives rise to the large variance for antenna 12 seen in figure 4.

Figure 6: The phase of the standing wave in the bandpass response function of antenna 12 as a function of time. The points represent the channel numbers of the 2 peaks in the bandpass (see figure 5). Values were taken from the bandpass solutions determined from each 10 minute scan on 3C 286 from the A/B array observations. The slope in each set of points is about -375 kHz/hour.

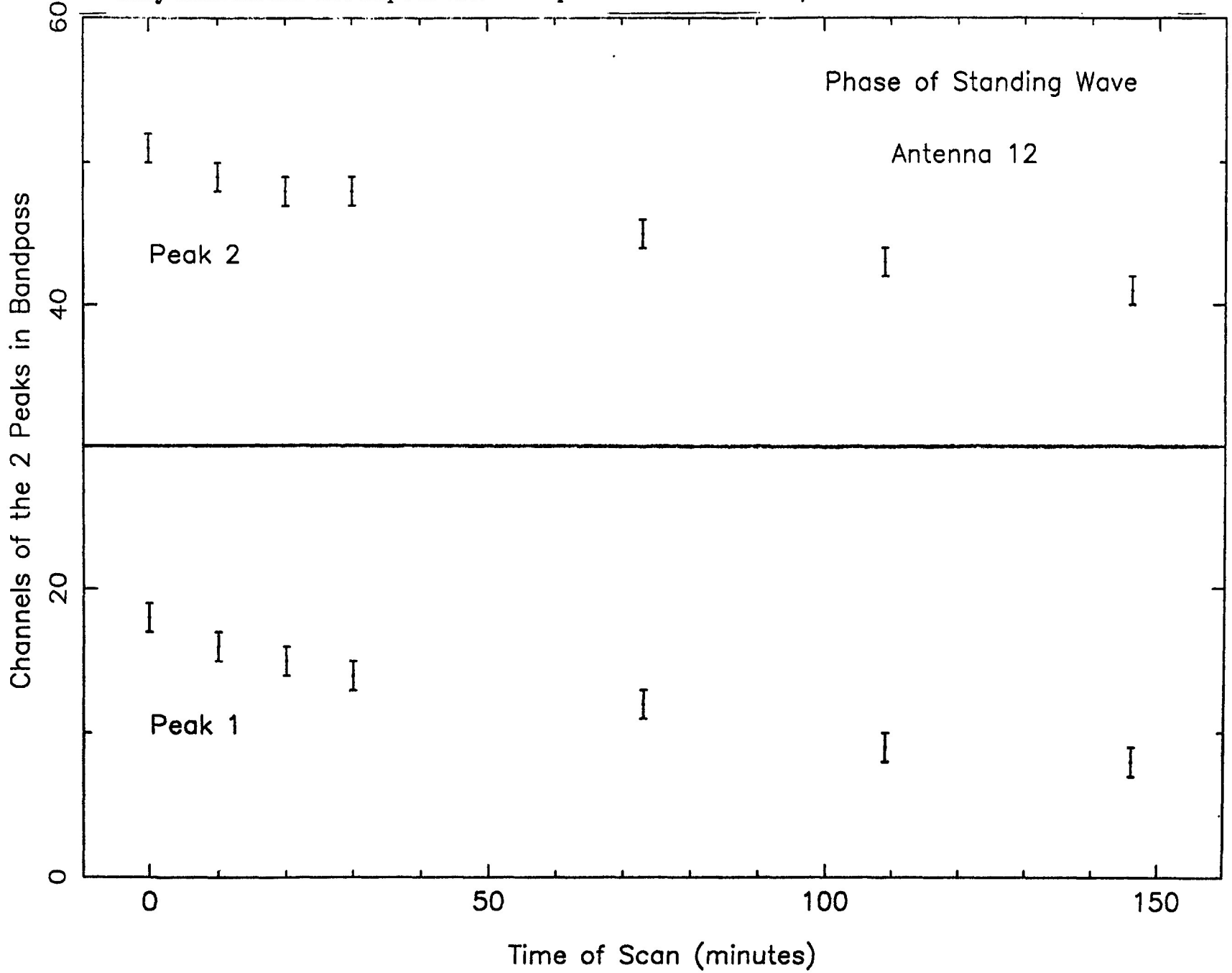

Figure 7: A. The peak to peak amplitude of the standing wave in the bandpass response function of antenna 12 over time. The data is the same as that for figure 6. B. The period of the standing wave of antenna 12 over time.

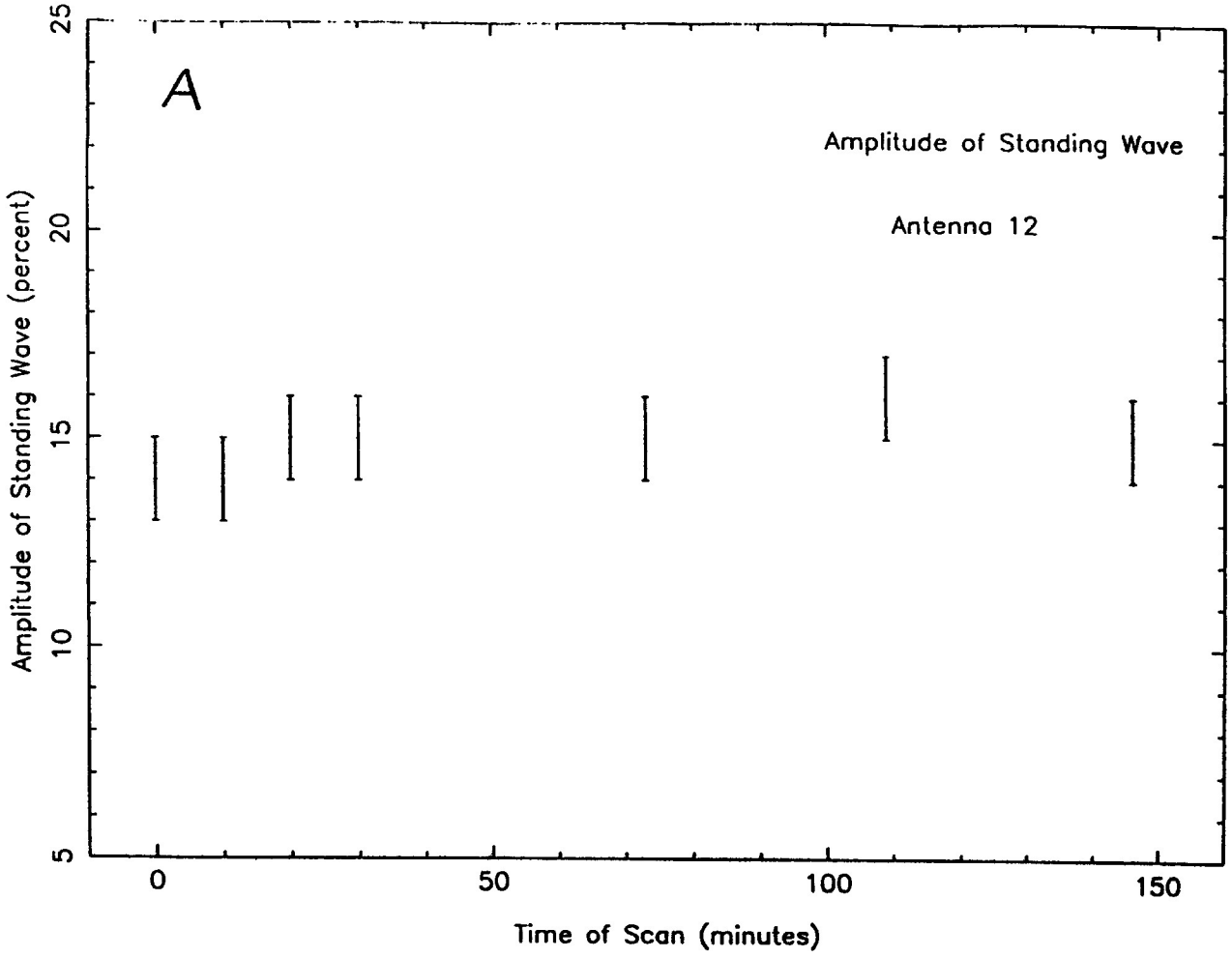
A
Amplitude of Standing Wave
Antenna 12
Amplitude of Standing Wave (percent)
25
20
15
10
5
0
50
100
150
Time of Scan (minutes)

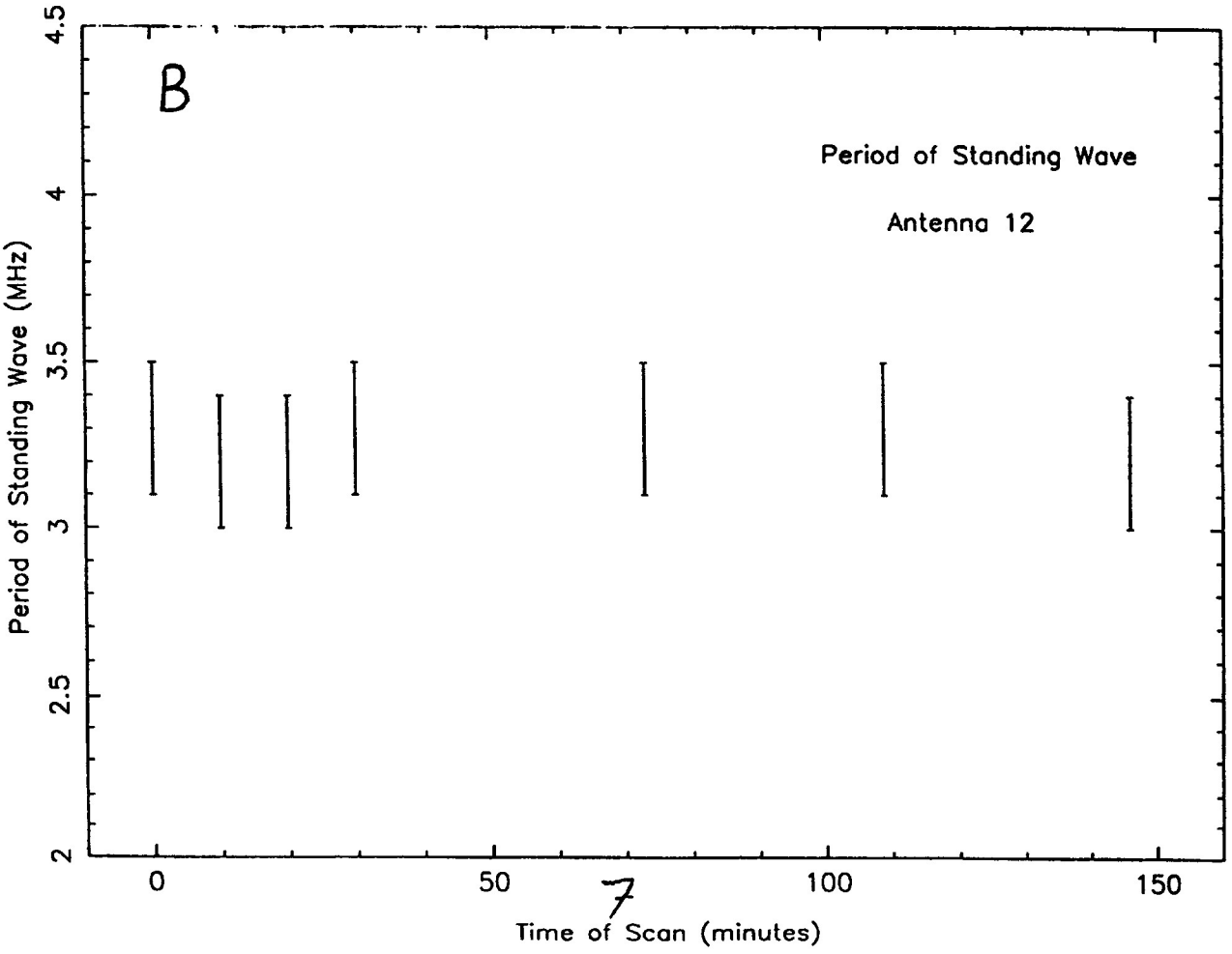
B
Period of Standing Wave
Antenna 12
Period of Standing Wave (MHz)
4.5
4
3.5
3
2.5
2
0
50
100
150
Time of Scan (minutes)

Figure 8: Same as figure 1, but with the bad antennas flagged. Notice the change in scale from figure 1 to figure 8.

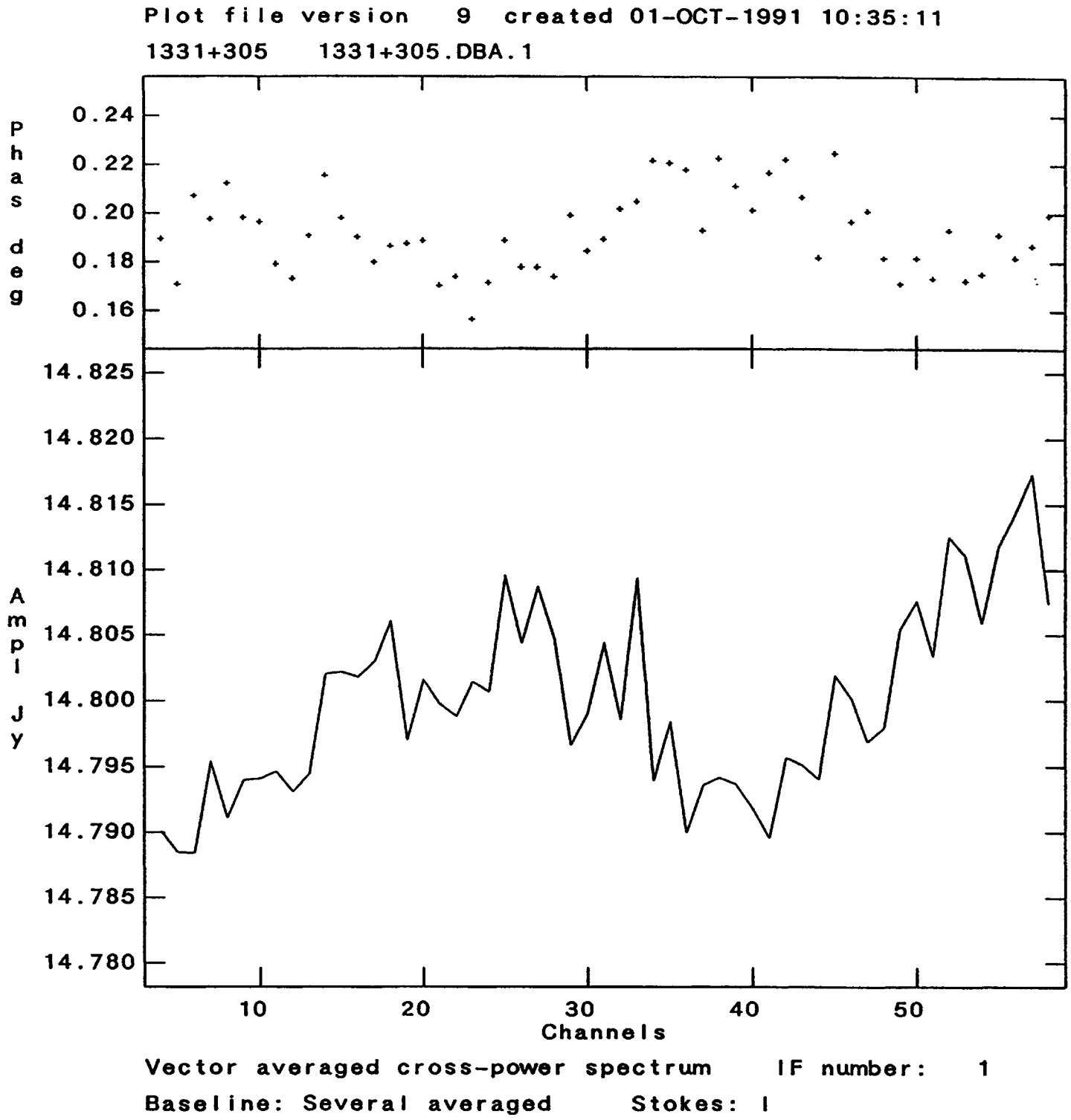

Figure 9: Same as figure 1, but with the bandpass response function of each telescope interpolated to the 'target' scan from a scan just prior to, and a scan just following, the 'target' scan. The scale is the same as figure 1. Notice the decrease in the residual ripple in the source spectrum.

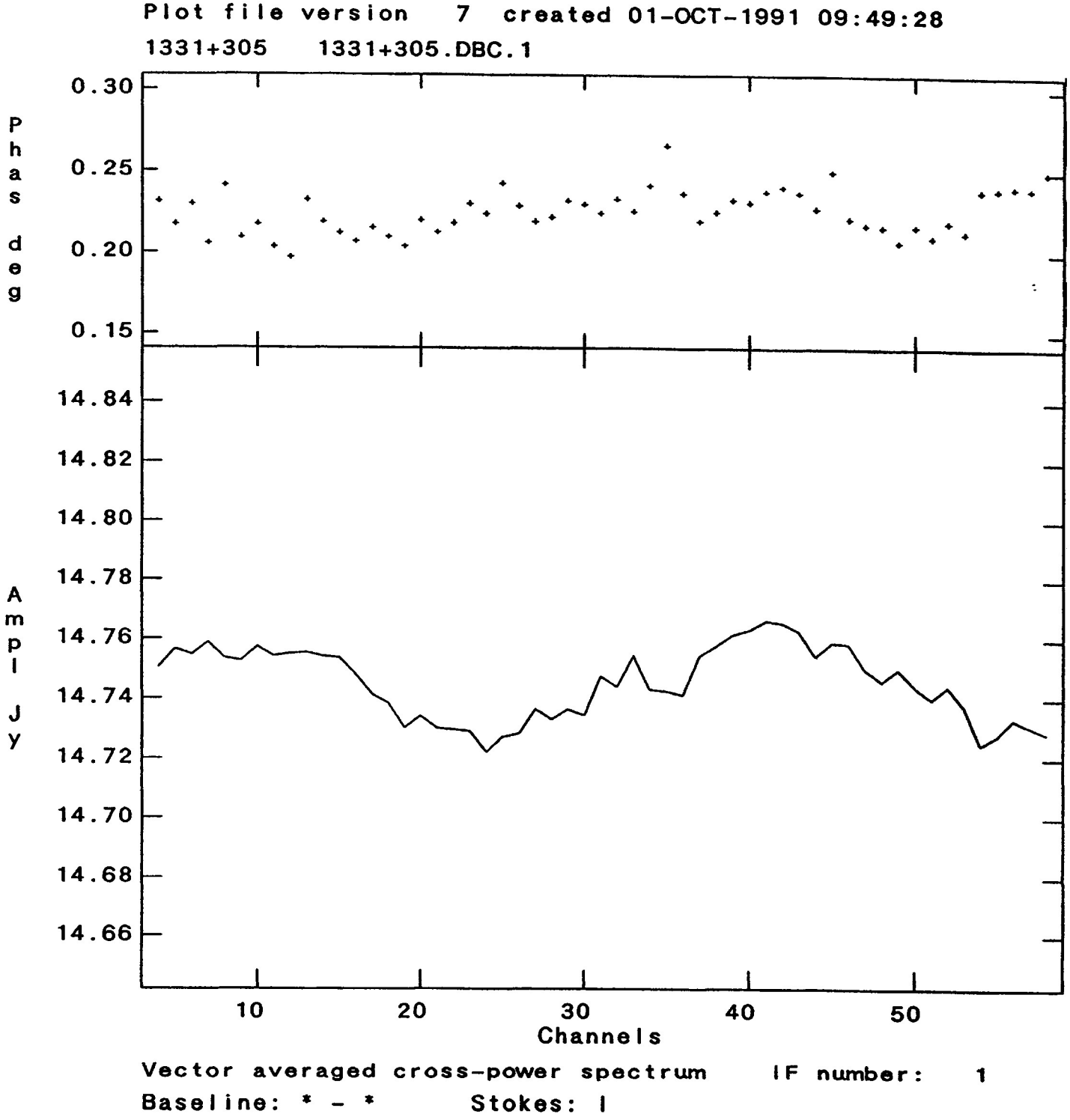

Figure 10: Same as figure 1, but with the bad antennas flagged and with the bandpass response function of each telescope interpolated to the 'target' scan from a scan just prior to, and a scan just following, the 'target' scan. This is on the same scale as figure 8. The measured noise on this spectrum is roughly equal to the expected theoretical noise of 6 mJy.

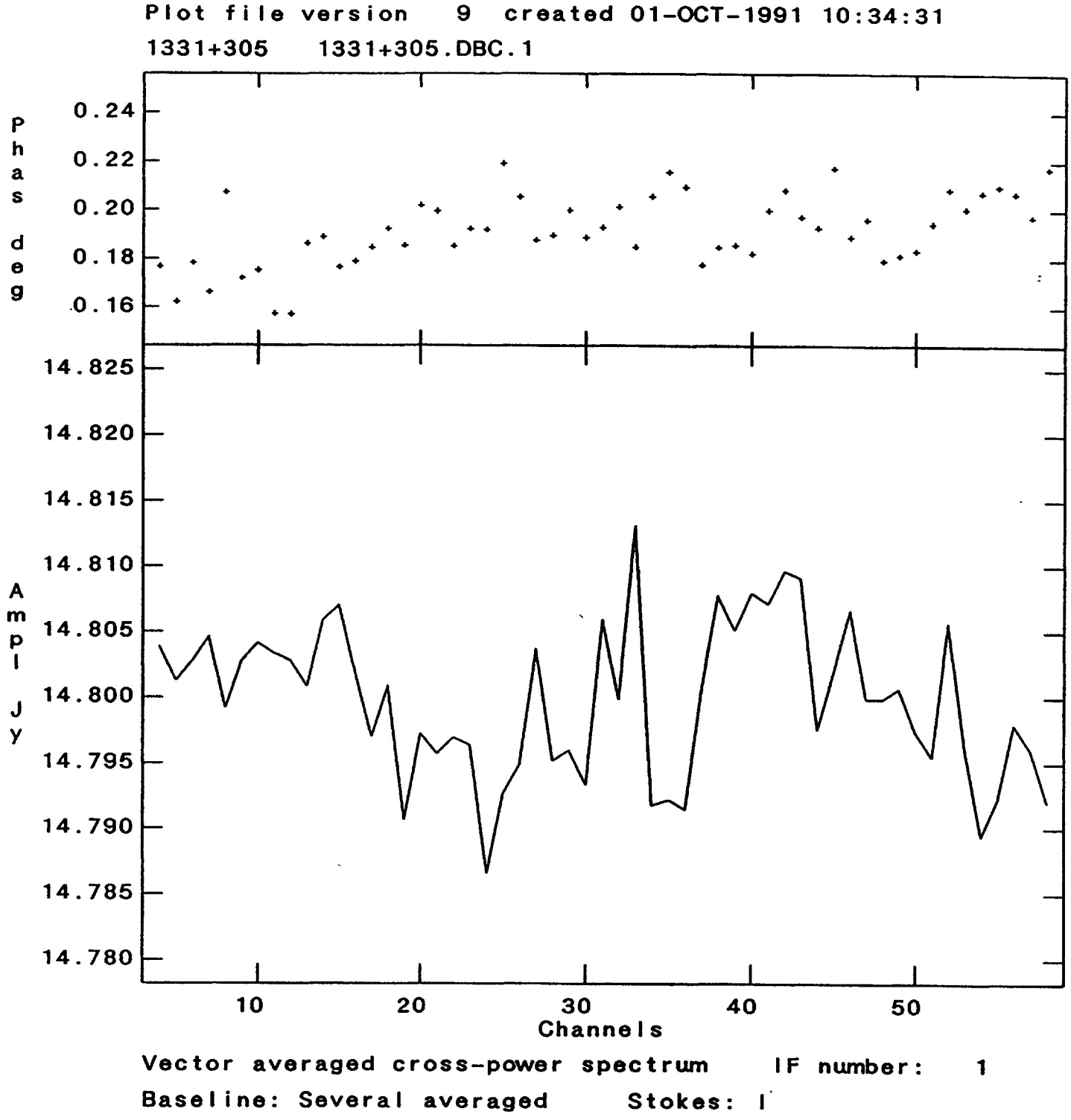

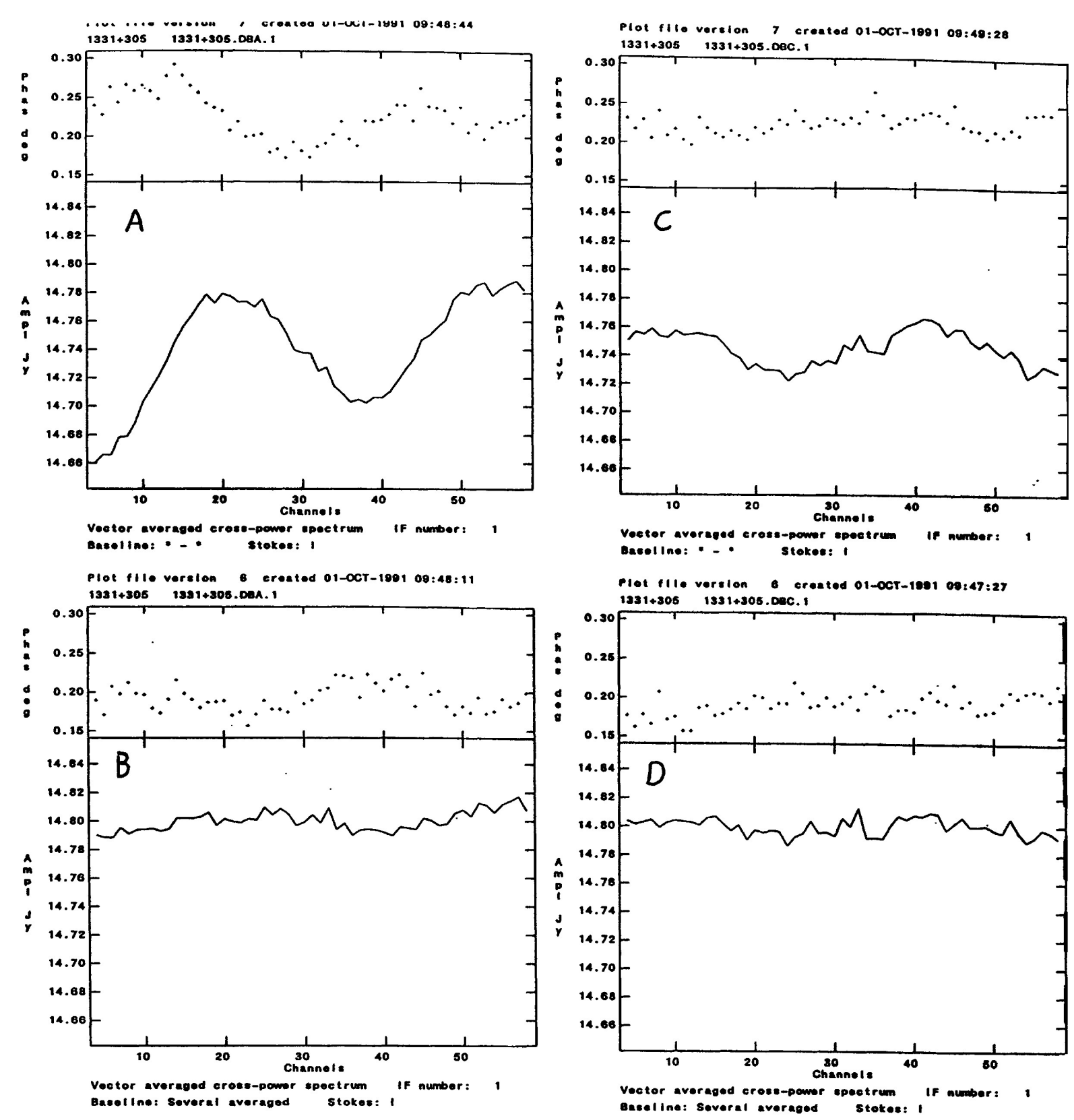

Figure 11: A composite of figures 1 (= A), 8 (= B), 9 (= C), and 10 (= D), showing the sequence of improvement in spectral dynamic range with flagging (B), bandpass interpolation (C), and both (D). All spectra are on the same scale. The original spectral dynamic range is 125 (spectrum A), and the final spectral dynamic range is $\geq$ 1500 (spectrum D).

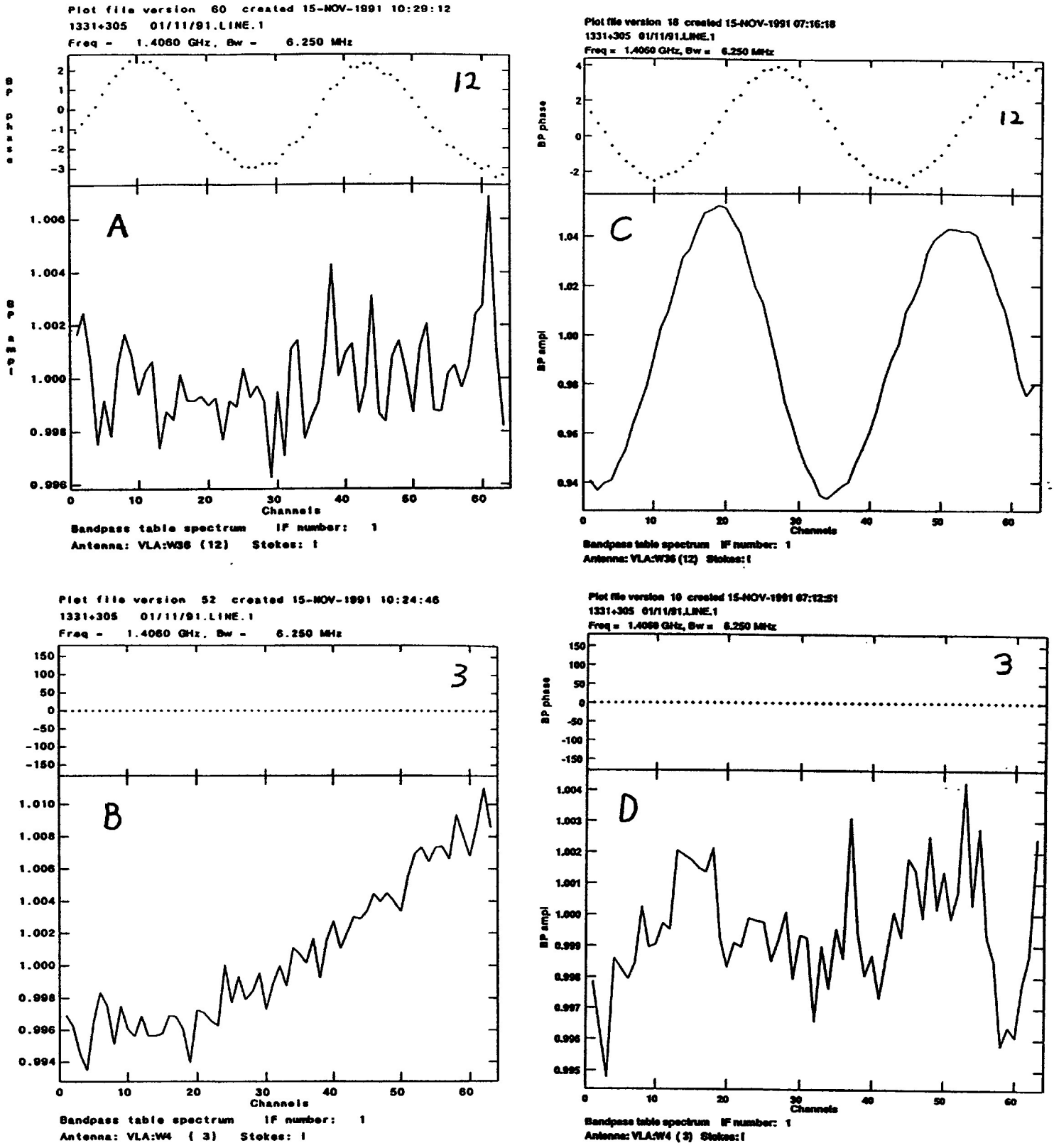

Figure A1: Bandpass variance plots for two antennas from the B array observations. Parts A and B are the variances for antennas 12 and 3 with auto-normalization applied. Parts C and D are the variances for antennas 12 and 3 without auto-normalization (see appendix).

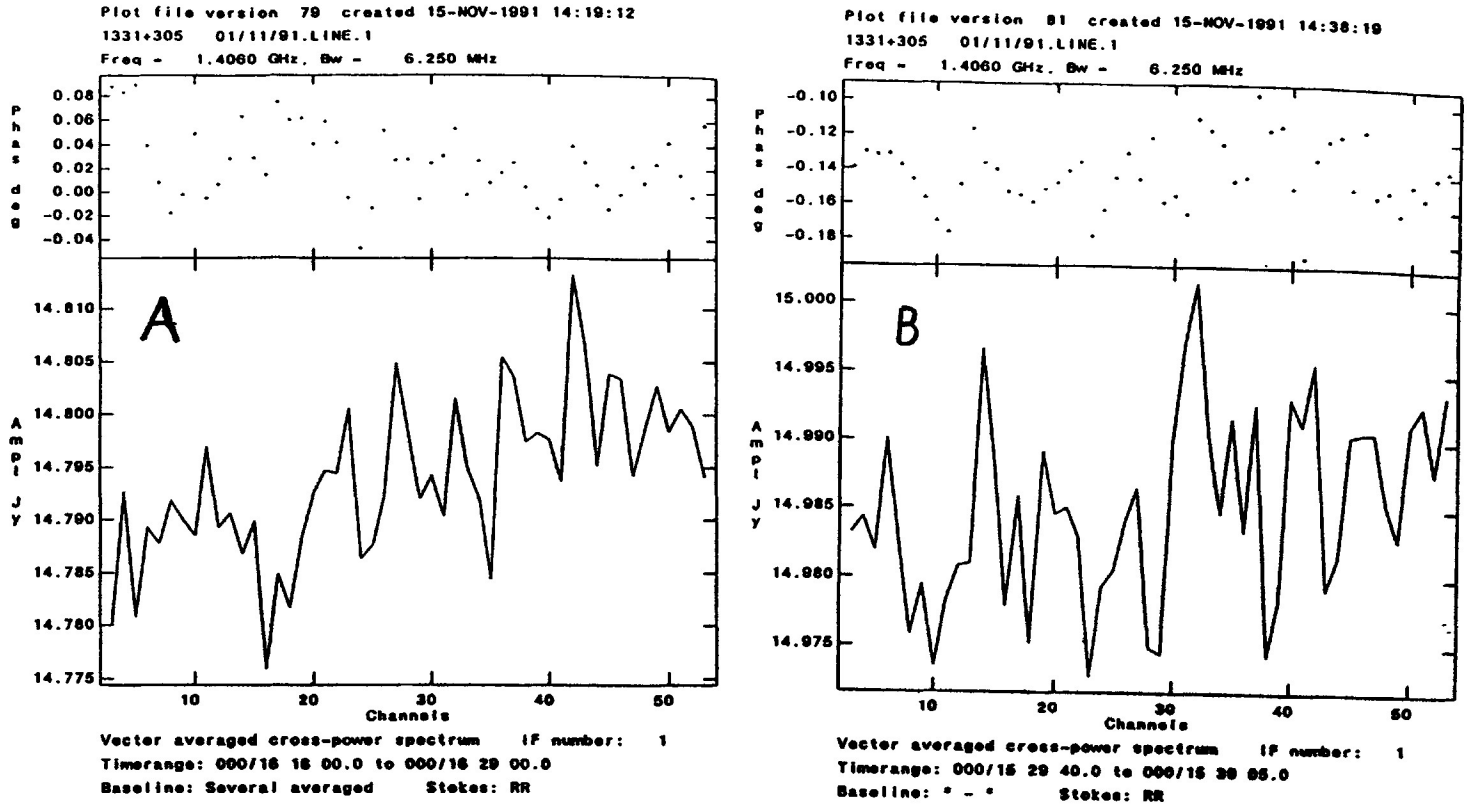

Figure A2: Spectra of 3C 286 made using the techniques described in section IV. Part A is a spectrum made in the normal fashion, *i.e.* without bandpass auto-normalization. Part B is a spectrum made with auto-normalization applied (see appendix).

These are appendices to VLA Test memorandum no. 158.

Appendix B. Source Changes

In this section we show that the temporal drift of the position of the 3.2 MHz bandpass ripple is continuous through source changes. Figure B1 shows bandpass solutions determined from a series of 12 minute scans from the B array observations of November 1991. Figure A shows 5 bandpass solutions for antenna 12, and figure B shows the same series of solutions for antenna 14. For these observations, antenna 12 shows a large variance in it's bandpass, while antenna 14 shows no variance to within the noise. The solutions for antenna 12 are labeled 1 through 5, with 1 being the solution from the first scan, and 5 being that from the last scan. The source observed for scans 1, 3, and 5 was 3C 286, while that for scans 2 and 4 was 3C 273.

For antenna 12, we see the characteristic 3.2 MHz ripple in the bandpass response function, and the smooth drift in the position of this ripple over time. The encouraging thing is that we see no discontinuity in this drift with source change. The rate of change for the position of the bandpass ripple for antenna 12 for this run is 1410 kHz/hr.

For antenna 14 (figure B), we find that the bandpass appears to be stable to within the noise throughout the observations and that the bandpass is not source dependent.

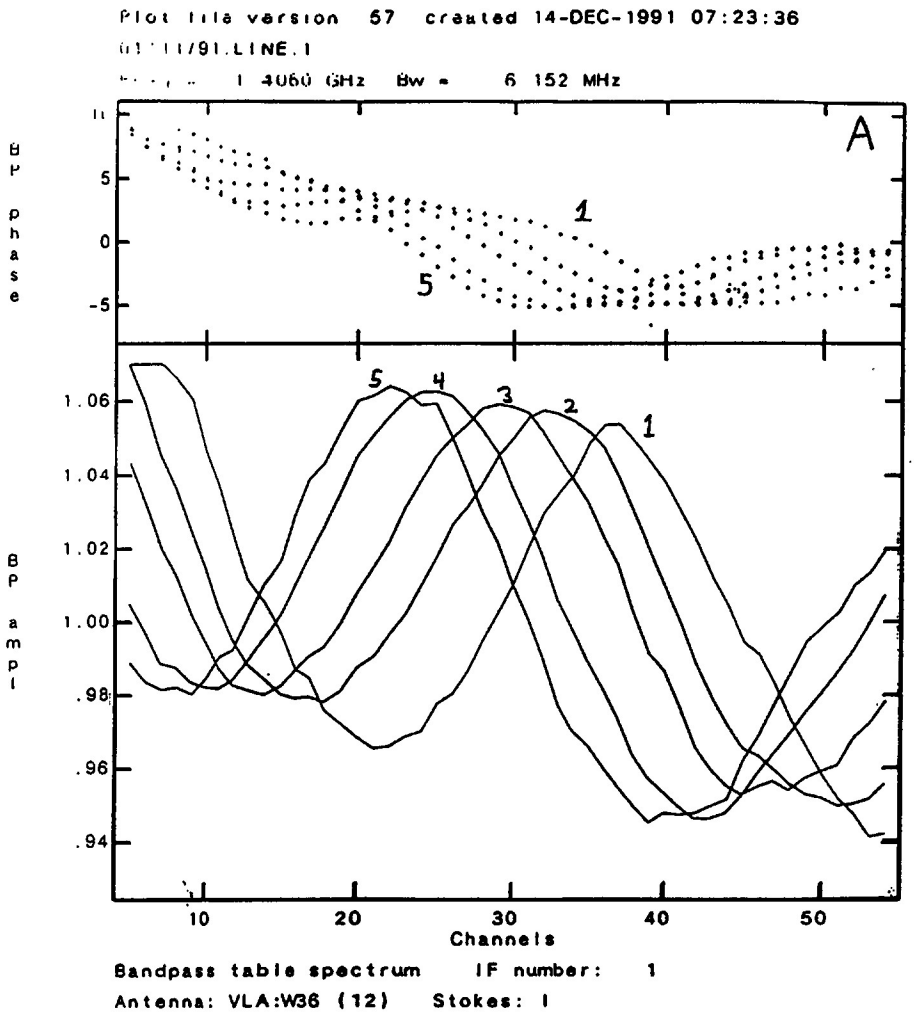

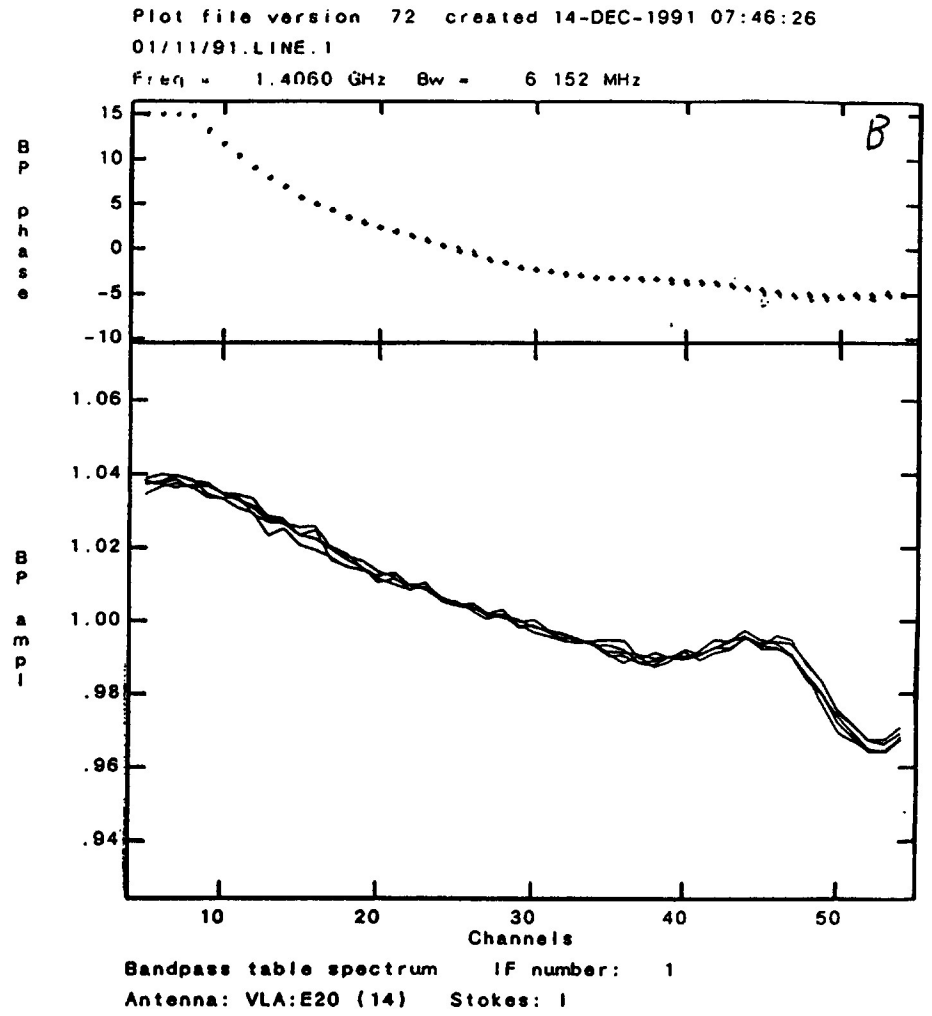

Figure B1-A: Bandpass solutions for antenna 12 from a series of 12 minute scans, labeled 1 through 5 from data taken in November, 1991. The observed source for solutions 1, 3, and 5 was 3C 286, while that for solutions 2 and 4 was 3C 273. The observing frequency was 1406 MHz and the channel width was 97.7 kHz.

Figure B1-B: The same series of bandpass solutions as figure B1-A, but now for antenna 14.

Appendix C: Other Bands

In this section we show that the 3.2 MHz ripple is not isolated to L band. These test observations were made on December 27, 1991 in B array. The procedure was the same as that for previous observations, but included scans at C band (4885 MHz) and X band (8085 MHz).

In figure C1 we show bandpass solutions for 2 scans on 3C 286 at L band. The scans are separated in time by 23 minutes. Figure A shows solutions for antenna 12, while figure B shows solutions for antenna 1. Antenna 12 shows a large bandpass variance for this run, while antenna 1 shows no variance to within the noise. For antenna 12 we see the characteristic 3.2 MHz ripple in the bandpass response function, and the drift of the position of this ripple with time.

In figures C2 and C3 we show bandpass solutions for 2 scans on 3C 286, again for antennas 12 and 1 (figures A and B, respectively). Figure C2 is for data taken at X band, and the 2 scans are separated in time by 55 minutes. Figure C3 is for data taken at C band, and the 2 scans are separated in time by 42 minutes. At both X and C band, antenna 12 shows a large bandpass variance for these observations, while antenna 1 shows no variance to within the noise. For antenna 12 we see again the 3.2 MHz ripple in the bandpass response function, at both X and C band, and we see the drift in position of this ripple over time.

A detailed look at the bandpass variances for each antenna at each band shows that antenna characteristics do not change with band, *i.e.* for a given observing run, the 'bad' antennas are bad at L, X, and C bands. We find no continuity in the position of the bandpass ripple between frequency changes. The rate for the drift in position of the ripple for these observations is 460 $\pm$ 90 kHz/hr at L band, and 230 $\pm$ 50 kHz/hr at both X and C band (although the drift direction is reversed for C band with respect to X band).

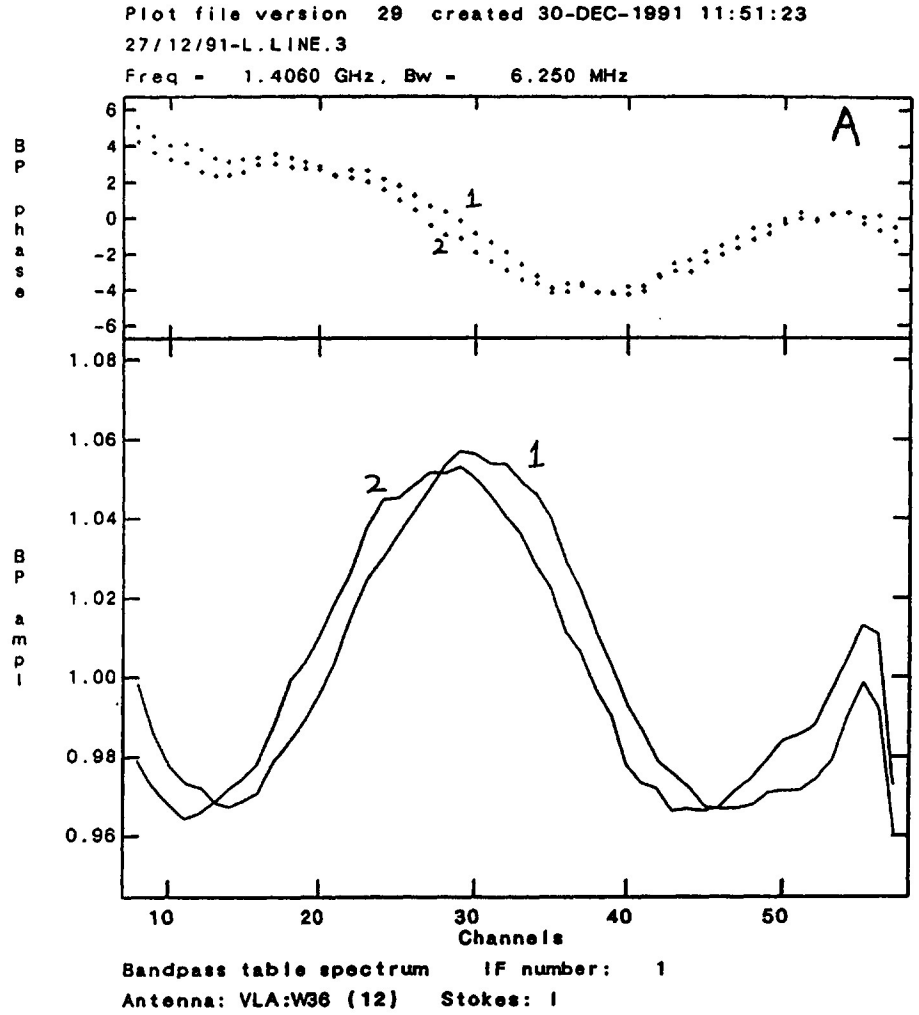

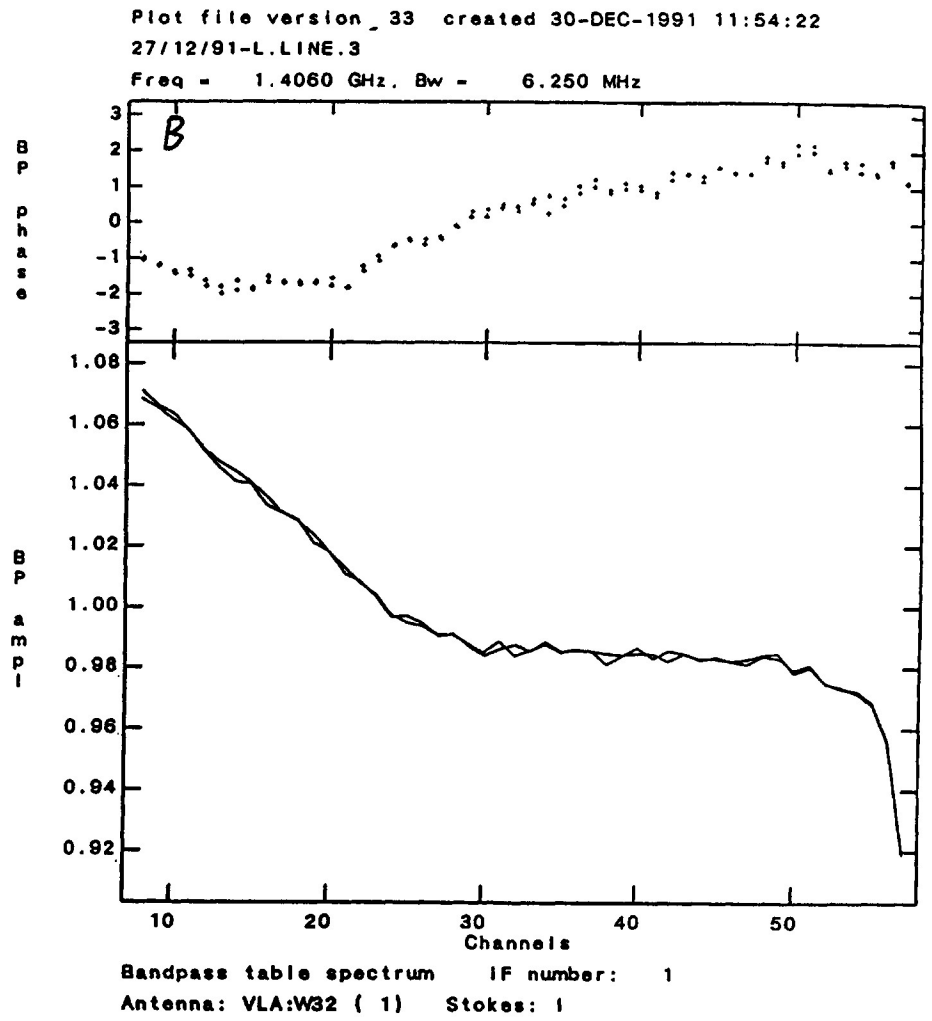

Figure C1-A: Bandpass solutions for antenna 12 from two scans on 3C 286 taken in December, 1991, separated by 23 minutes in time. The observing frequency was 1406 MHz and the channel width was 97.7 kHz.

Figure C1-B: The same as figure C1-A, but for antenna 1.

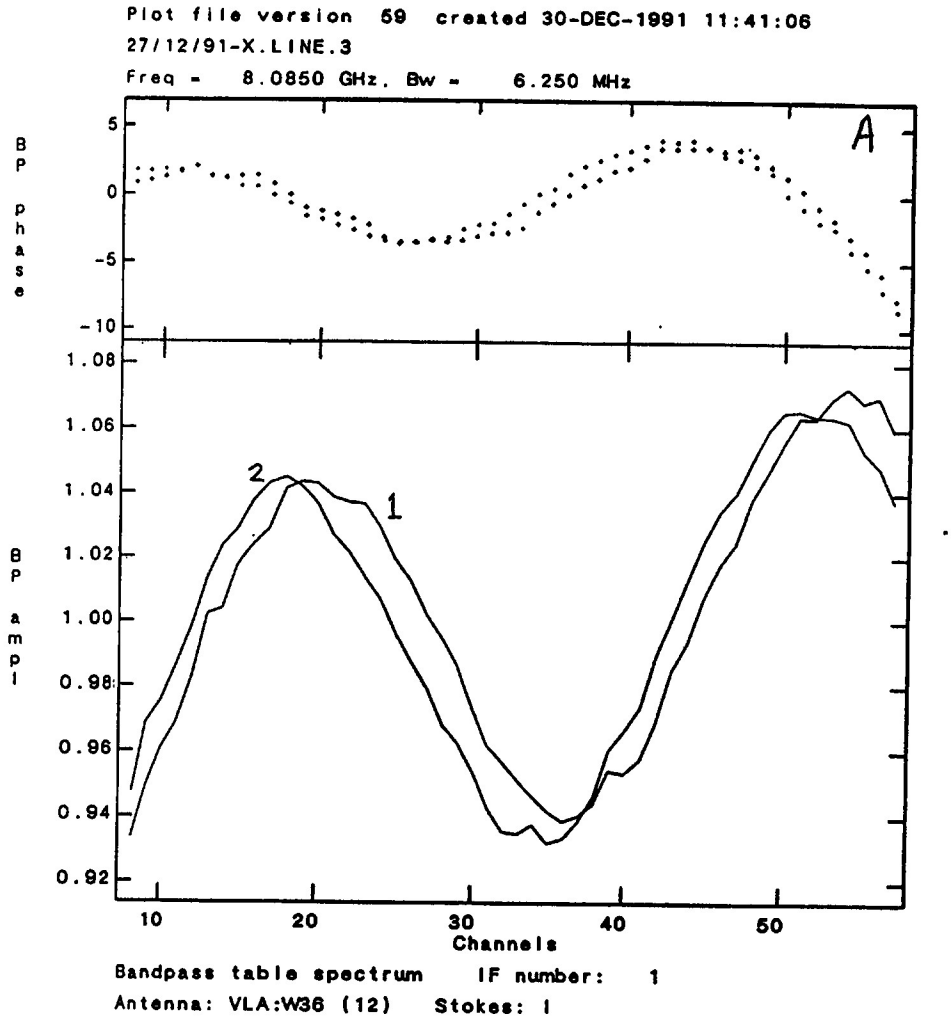

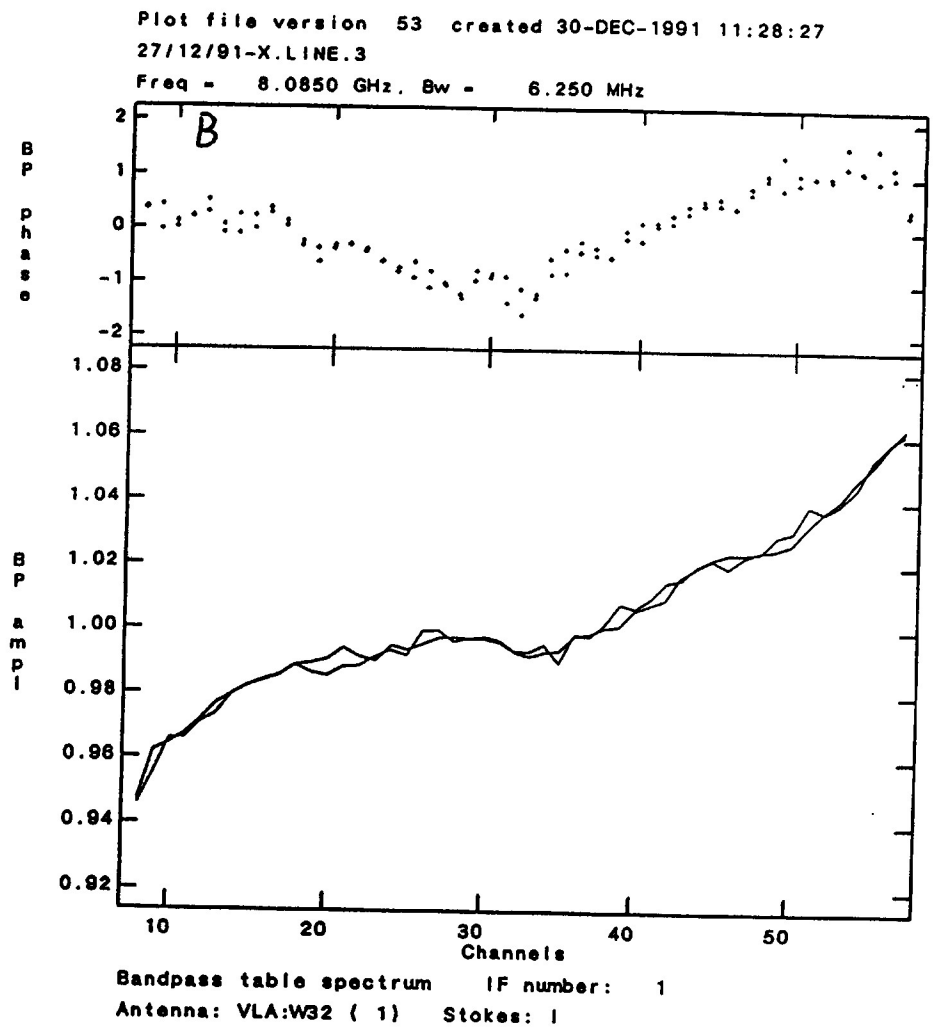

Figure C2-A: Bandpass solutions for antenna 12 from two scans on 3C 286 taken in December, 1991, separated by 55 minutes in time. The observing frequency was 8085 MHz and the channel width was 97.7 kHz.

Figure C2-B: The same as figure C2-A, but for antenna 1.

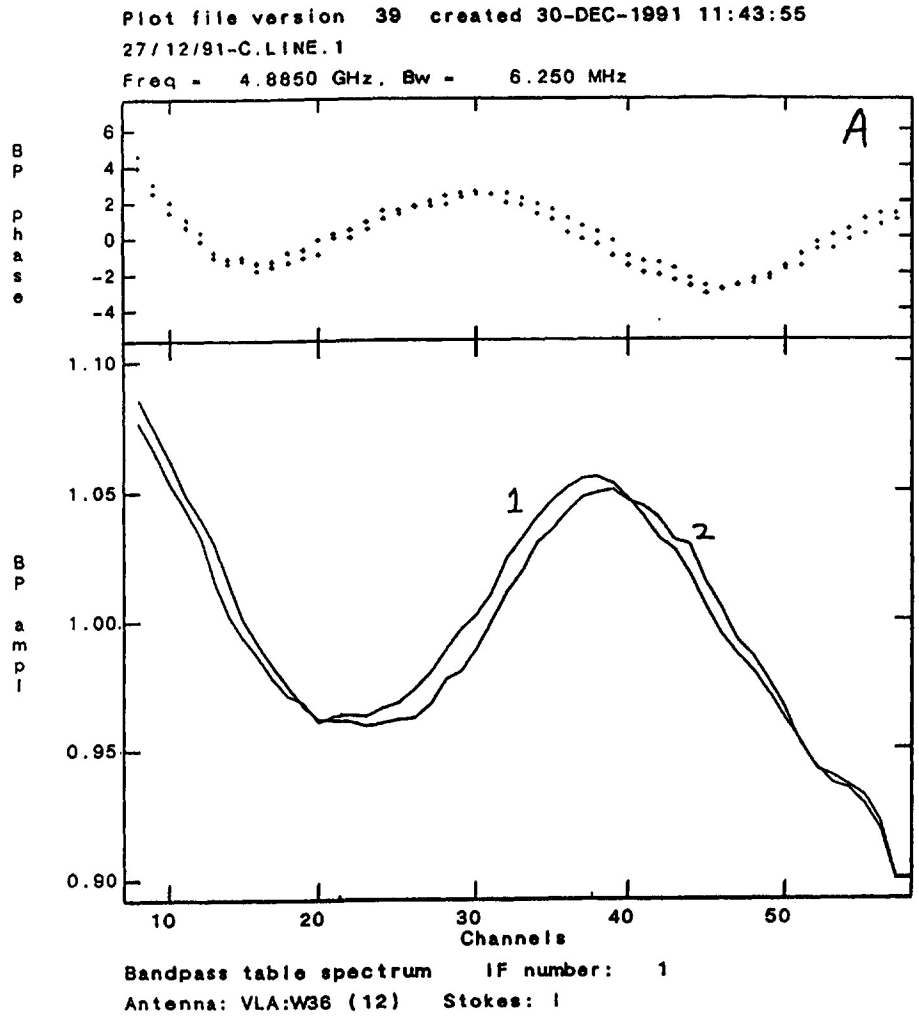

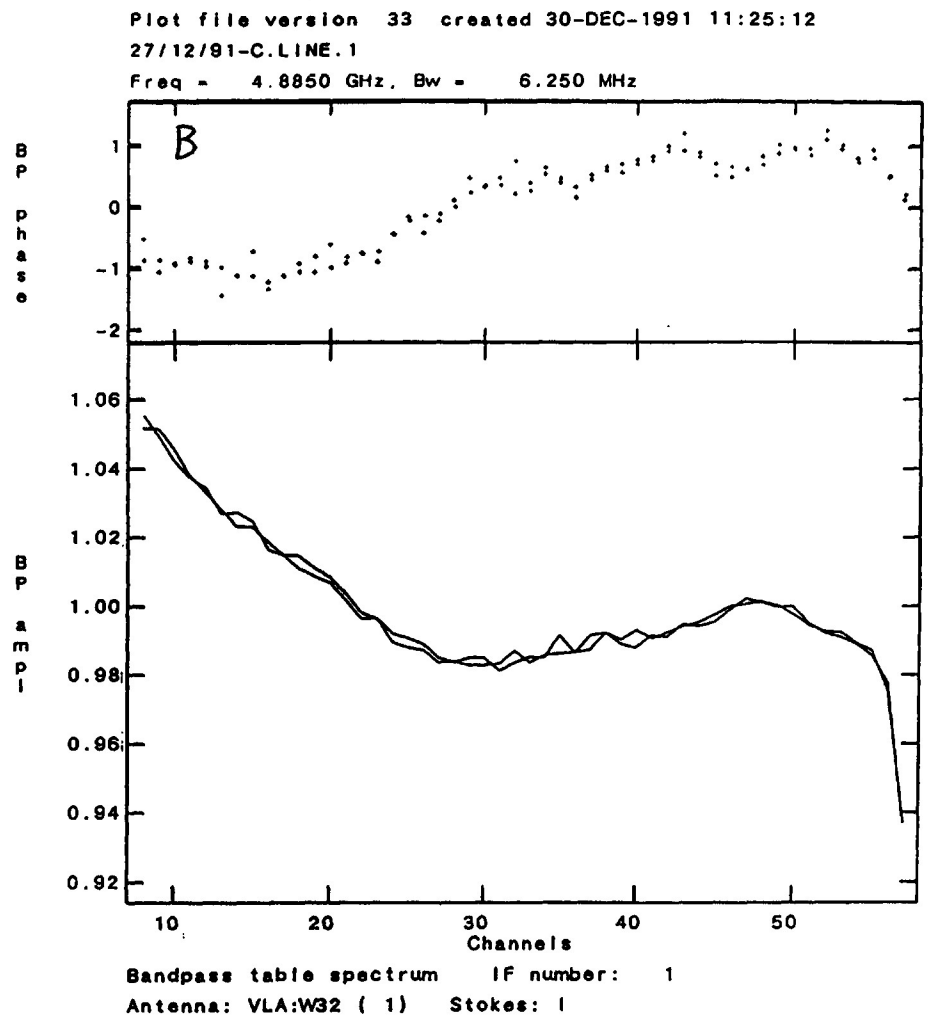

Figure C3-A: Bandpass solutions for antenna 12 from two scans on 3C 286 taken in December, 1991, separated by 43 minutes in time. The observing frequency was 4885 MHz and the channel width was 97.7 kHz.

Figure C3-B: The same as figure C3-A, but for antenna 1.

These are more appendices to VLA Test memorandum no. 158, 'Spectral Dynamic Range at the VLA', by Chris Carilli. These appendices were added on May 6, 1992.

Appendix D: Attenuation and Mode Suppression

We show that the ripple in the spectral response function of antenna 12 is due to a standing wave in the 20mm circular waveguide. The test procedure is exactly the same as that discussed in section II of the memo. Test observations were made in C array on April 5, 9, and 22 1992.

Figure D1 shows the bandpass for antenna 12 from a single 15 minute scan from the April 5 observations. Figure D2 shows the bandpass for antenna 12 from a single 15 minute scan from the April 9, 1992 observations. The standing wave in the bandpass response for antenna 12 is seen clearly in the observations of April 5. On April 9, the standing wave in the bandpass response of antenna 12 is not seen.

Why was there a change between April 5 and 9? A 6 dB attenuator was inserted into the 20mm waveguide of antenna 12 during maintenance day (April 7, 1992). This device will attenuate reflected signal, thereby decreasing standing waves and the frequency dependent gain variations associated with them. The predicted behavior is born out by observation. This implies that the bandpass ripple is indeed a standing wave, and that the standing wave is indeed located in the antenna's 20mm waveguide.

The variances of the bandpass for antenna 12 for these two dates are shown in figures D3 and D4. The variance on April 5 shows the familiar signature of the 3.2 MHz standing wave which shifts in phase over time. The variance on April 9 is an order of magnitude smaller than on April 5, and it shows no sign of the 3.2 MHz ripple, as expected.

Inspection of the bandpass shapes and variances for all antennas besides 12 shows behavior consistent with essentially no change to the rest of the system between April 5 and April 9. Hence, the change in the bandpass for antenna 12 is a direct result of the attenuator.

We note that the modem in antenna 12 was changed in March, 1992. Comparison of data taken before and after the swap shows that the modem change did not affect the bandpass ripple.

Between observations on April 9 and April 22, the attenuator in antenna 12 was removed and a mode suppressor was inserted in the same place. The hope was that reflection may also cause mode conversion, and hence a mode suppressor might have the same effect on the standing wave as the attenuator, without the unwanted effect of decreasing the signal-to-noise. Figure D5 shows the bandpass of antenna 12 after the swap. The standing wave is back, with essentially the same amplitude as for the April 5 observations, *i.e.* before the attenuator was installed.

Figure D1: The bandpass of antenna 12 for data taken on April 5, 1992 (before inserting a 6 dB attenuator in the 20mm waveguide of antenna 12). Each channel has a width of 97.656 MHz. This bandpass was made from a 15 minute scan on 3C 286. The observing frequency was 1406 MHz.

Figure D2: The bandpass of antenna 12 for data taken on April 9, 1992 (after inserting a 6 dB attenuator in the 20mm waveguide of antenna 12). This bandpass was made from a single 15 minute scan on 3C 286.

Figure D3: The bandpass variance of antenna 12 for data taken on April 5, 1992. The variance was determined using two scans of fifteen minute duration, separated by 60 minutes in time.

Figure D4: The bandpass variance of antenna 12 for data taken on April 9, 1992. The variance was determined using two scans of fifteen minute duration, separated by 60 minutes in time.

Figure D5: The bandpass of antenna 12 for data taken on April 22, 1992 (after removing the attenuator and inserting a mode suppressor). This bandpass was made from a single 15 minute scan on 3C 286.

D 1

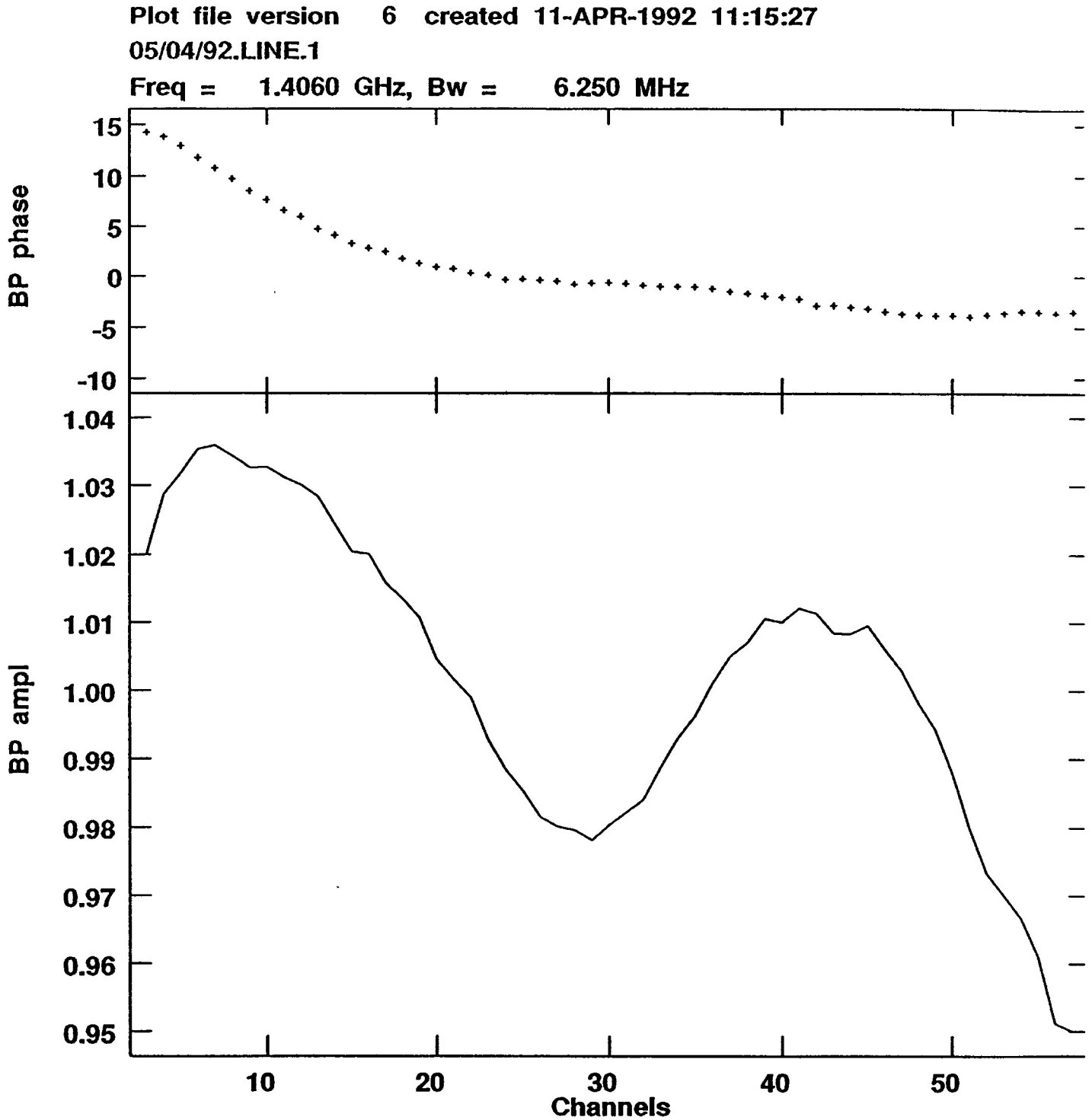
Plot file version 6 created 11-APR-1992 11:15:27
05/04/92.LINE.1
Freq = 1.4060 GHz, Bw = 6.250 MHz
BP phase
15
10
5
0
-5
-10
BP ampl
1.04
1.03
1.02
1.01
1.00
0.99
0.98
0.97
0.96
0.95
10
20
30
40
50
Channels
Bandpass table spectrum IF number: 1
Antenna: VLA:W18 (12) Stokes: I

D2

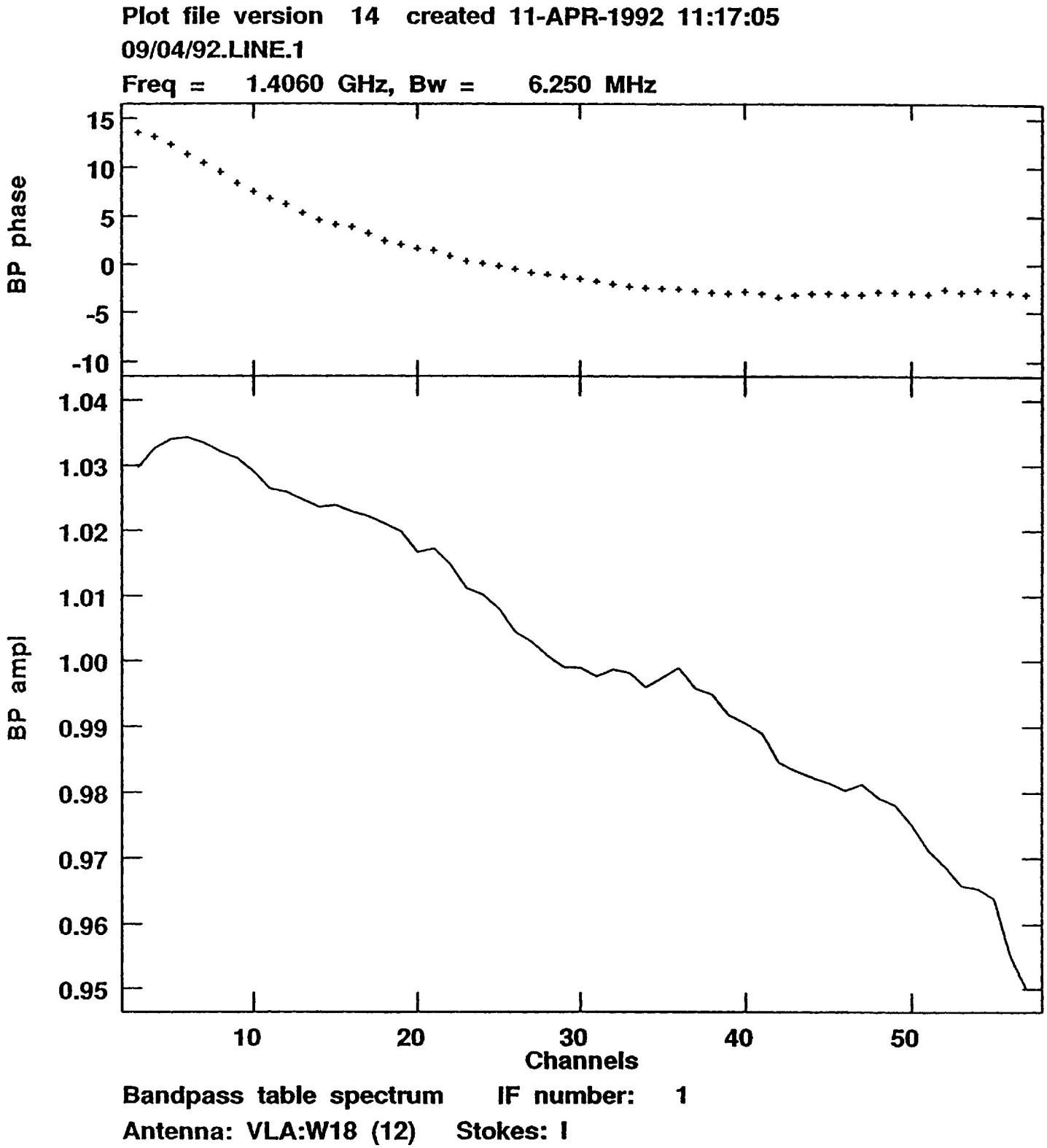
Plot file version 14 created 11-APR-1992 11:17:05
09/04/92.LINE.1
Freq = 1.4060 GHz, Bw = 6.250 MHz
BP phase
15
10
5
0
-5
-10
BP ampl
1.04
1.03
1.02
1.01
1.00
0.99
0.98
0.97
0.96
0.95
10
20
30
40
50
Channels
Bandpass table spectrum IF number: 1
Antenna: VLA:W18 (12) Stokes: I

D3

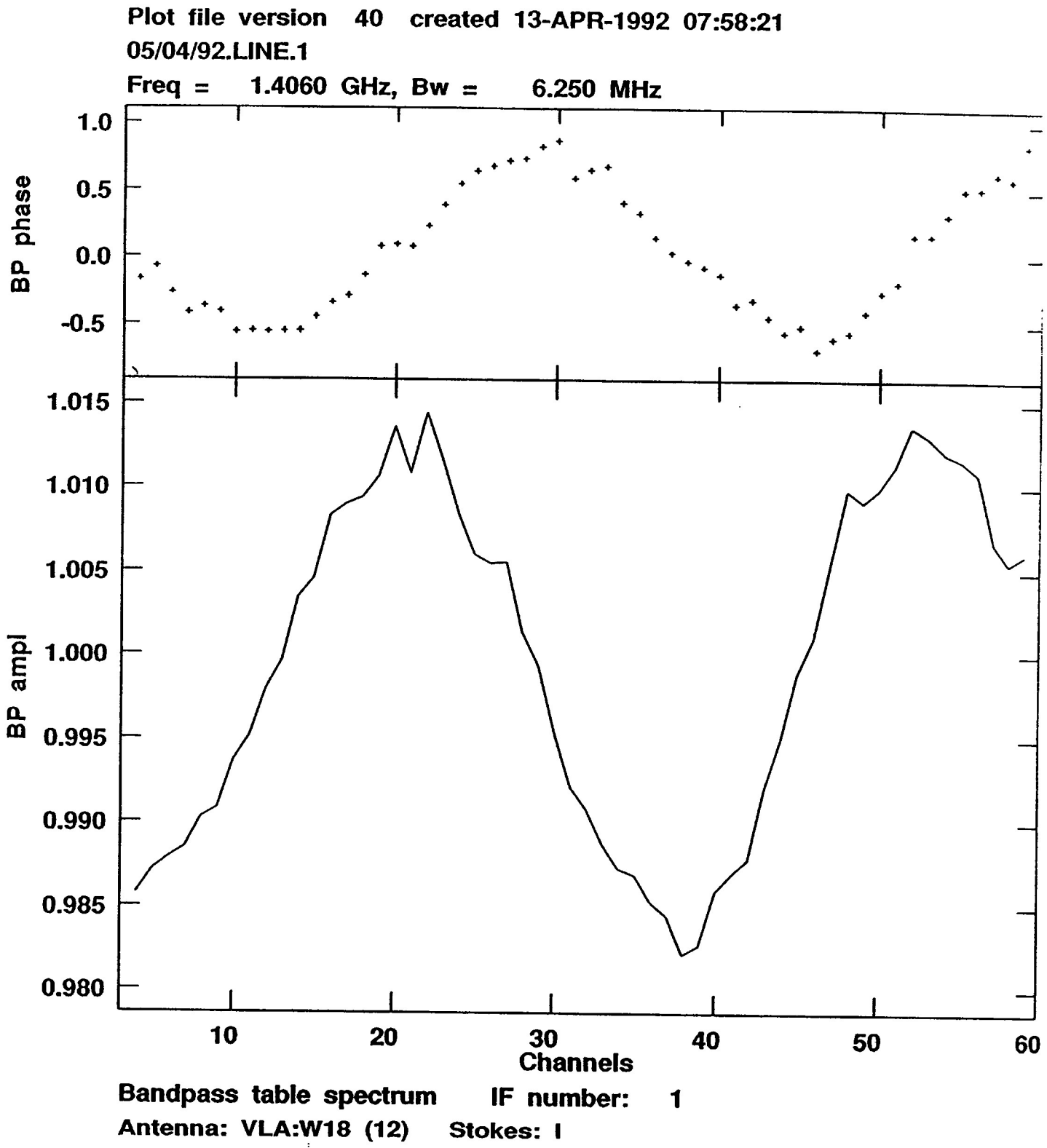
Plot file version 40 created 13-APR-1992 07:58:21
05/04/92.LINE.1
Freq = 1.4060 GHz, Bw = 6.250 MHz
BP phase
1.0
0.5
0.0
-0.5
BP ampl
1.015
1.010
1.005
1.000
0.995
0.990
0.985
0.980
10
20
30
40
50
60
Channels
Bandpass table spectrum IF number: 1
Antenna: VLA:W18 (12) Stokes: I

D4

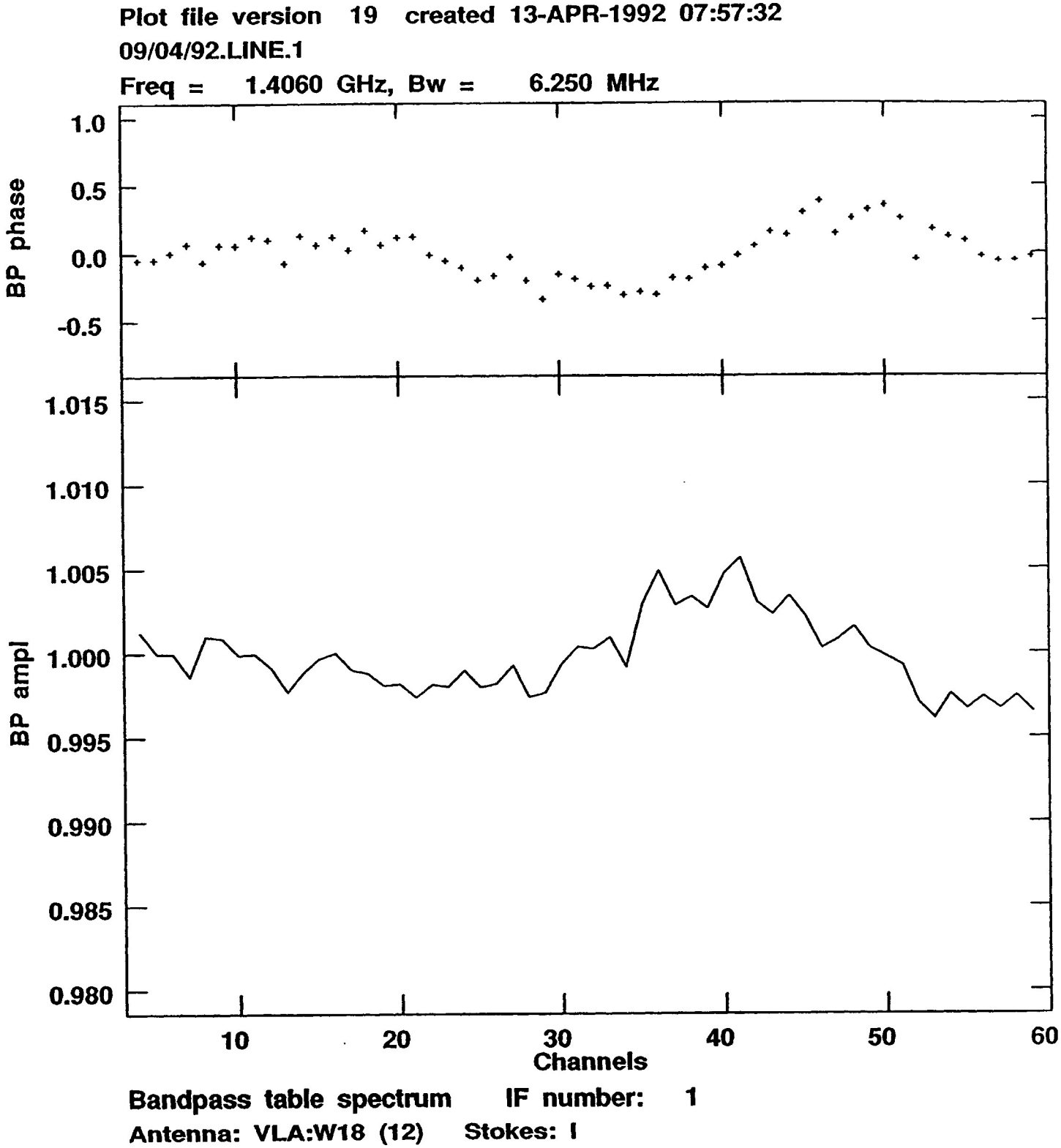
Plot file version 19 created 13-APR-1992 07:57:32
09/04/92.LINE.1
Freq = 1.4060 GHz, Bw = 6.250 MHz
BP phase
1.0
0.5
0.0
-0.5
BP ampl
1.015
1.010
1.005
1.000
0.995
0.990
0.985
0.980
10
20
30
40
50
60
Channels
Bandpass table spectrum IF number: 1
Antenna: VLA:W18 (12) Stokes: I

D 5

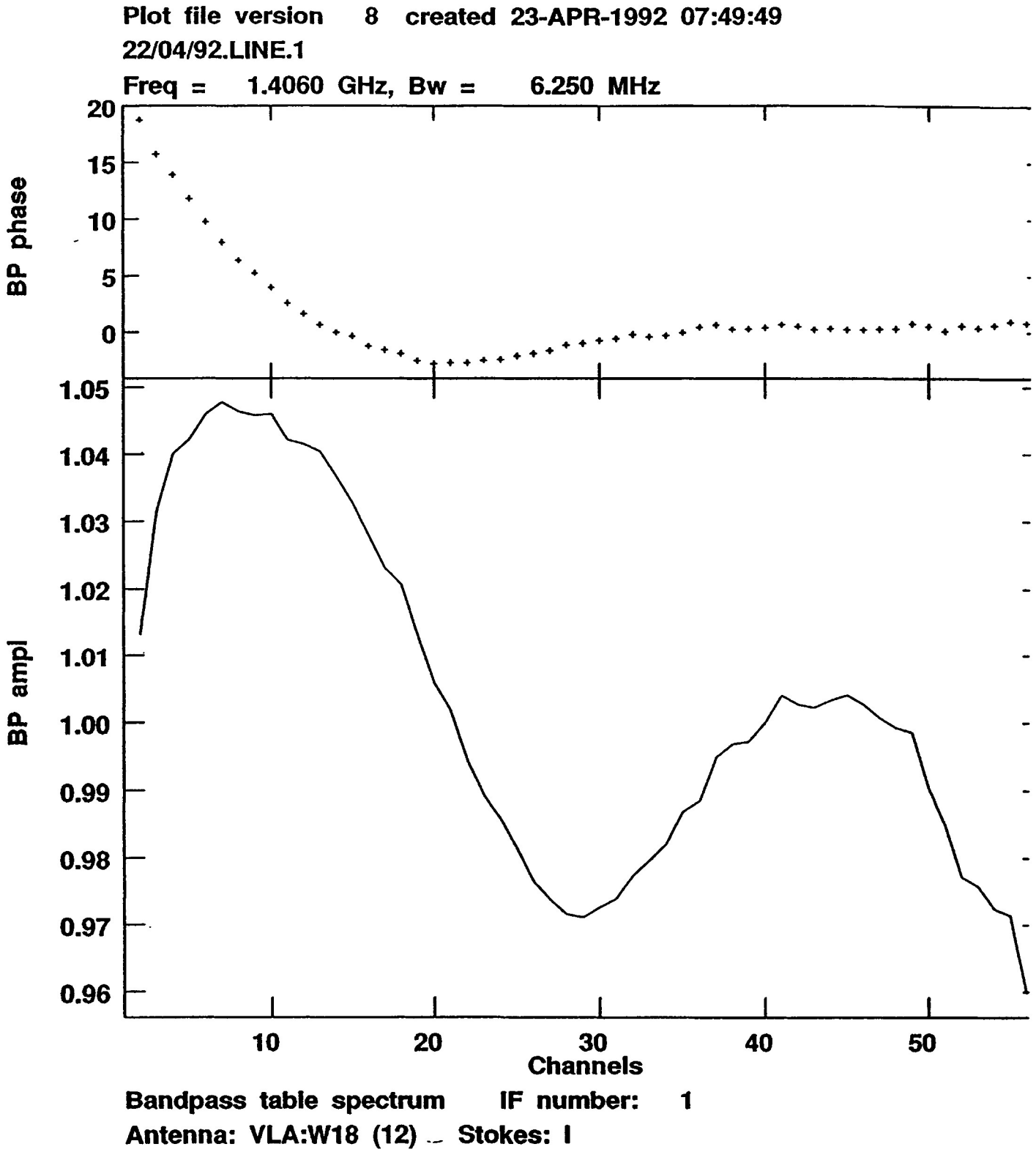
Plot file version 8 created 23-APR-1992 07:49:49
22/04/92.LINE.1
Freq = 1.4060 GHz, Bw = 6.250 MHz
BP phase
20
15
10
5
0
BP ampl
1.05
1.04
1.03
1.02
1.01
1.00
0.99
0.98
0.97
0.96
10
20
30
40
50
Channels
Bandpass table spectrum IF number: 1
Antenna: VLA:W18 (12) Stokes: I